αIIb(D163A) mutant (Fig. 2*B*). However, integrin αIIb deficiency did not affect surface expression levels of integrin αVβ3 in platelets (data not shown). These results suggested that regulatory mechanisms on surface expression levels of integrin αVβ3 differed between mast cells and platelets. One possible explanation is as follows: integrin αIIb deficiency might fail to influence surface expression levels of integrin αVβ3 if integrin β3 expression were sufficient in platelets, whereas it might promote the association of integrin αV with integrin β3 if integrin β3 expression were insufficient in mast cells. Further examination is necessary to fully understand the mechanism. Importantly, all the functional analyses (Figs. 2–4) showed that higher surface expression levels of integrin αVβ3 in integrin αIIb-deficient BMMCs enhanced adhesion to VN or vWF but did not compensate for the loss of mast-cell functions through interaction with FB. Based on this, we compared *in vivo* mast cell functions between WT and integrin αIIb-deficient mice.

First, integrin αIIb deficiency did not affect mast-cell numbers in tissues under normal conditions (Table 1). This seems reasonable, given that FB is not abundant outside blood vessels under normal conditions. Second, integrin αIIb deficiency did not affect two types of PCA estimated by ear dye extravasation or swelling (data not shown), which was reported to be mast cell-dependent (32–34). These results indicate that extravascular FB and fibrin accompanied by acute inflammation are unable to enhance mast-cell functions. On the other hand, recent advances demonstrate that FB is a central regulator of the inflammatory response as well as of hemostasis. Analysis of gene-targeted mice expressing a mutant form of FB, lacking the integrin $\alpha_M\beta2$-binding motif, demonstrated that the high affinity engagement of FB by integrin $\alpha_M\beta2$ in neutrophils and macrophages was critical for inflammatory responses (38, 39). Therefore, we speculated that FB extravasated at acute inflammatory sites activated neutrophils and macrophages via integrin $\alpha_M\beta2$ but failed to enhance mast-cell functions via integrin αIIbβ3. In contrast, we found striking differences between WT and integrin $\alpha IIb^{-/-}$ mice in FB-induced chronic inflammation: integrin αIIb deficiency strongly suppressed the increase of total inflammatory cells with mastocytosis in the peritoneal cavities. However, administration of single dose FB did not lead to any significant difference of initial inflammatory responses in these mice 24 h after inoculation (data not shown), confirming the negligible role of integrin αIIb in acute inflammation. Taking into consideration that platelets are absent in the peritoneal cavities and that integrin αVβ3 did not significantly affect *in vitro* mast-cell functions through interaction with FB, we concluded that FB-induced chronic inflammation depended on integrin αIIbβ3 in mast cells. The relevant mechanism might be as follows: FB activates macrophages and granulocytes via integrin $\alpha_M\beta2$ to produce inflammatory cytokines and chemokines in the initial phase, leading to the gradual recruitment, proliferation, and activation of mast cells in the presence of FB. Alternatively, activated mast cells also produce a diverse array of chemical mediators, accelerating chronic inflammation. Thus, FB-mediated inflammation appears to be augmented with the increase of mast cells in tissues. This scenario may explain in part why mast cell numbers increase in a variety of chronic inflammatory diseases such as atopic dermatitis and asthma that are thought to cause continuous extravasation of FB in tissues. Further analysis of WT and integrin αIIb-deficient mice using different types of chronic inflammation models will be required to delineate the role of mast cell integrin αIIbβ3 in chronic inflammatory diseases.

Another important finding in this study was that soluble FB enhanced IL-6 production of WT, but not integrin αIIb-deficient, BMMCs in response to *S. aureus* (Cowan I) with FB-binding capacity. On the other hand, soluble FB failed to enhance IL-6 production of WT BMMCs stimulated by *E. coli* harboring no FB-binding capacity, LPS, or bacterial lipopeptide (Fig. 7*B* and data not shown). Because WT, but not integrin αIIb-deficient, BMMCs apparently kept a strong contact with aggregated *S. aureus* (Cowan I) in the presence of soluble FB, integrin αIIbβ3-dependent recognition of *S. aureus* (Cowan I) in mast cells may augment the innate response to this pathogen. Considering that soluble FB facilitates the interaction of platelets with *S. aureus* by bridging clumping factor A in *S. aureus* and integrin αIIbβ3 in platelets (23–25), a similar mechanism probably occurs in mast cells: the complex formation of mast cell integrin αIIbβ3-FB-*S. aureus* (Cowan I) promotes quick and tight recognition of this pathogen by mast cells, thereby enhancing innate immune responses. Collectively, these results suggested that integrin αIIbβ3 plays an important part in the innate responses of mast cells to certain types of bacteria with FB-binding capacity.

In conclusion, the integrin αIIbβ3-dependent interaction of mast cells with FB augments FB-associated chronic inflammation or innate responses to FB-binding bacteria. Elucidation of the *in vivo* function of integrin αIIbβ3 in mast cells will lead to new approaches in the prevention of and therapy for the relevant inflammatory and infectious diseases.

Acknowledgments—We thank Drs. B. S. Coller, V. L. Woods, D. J. Gerber, and S. Tonegawa for providing Abs. We thank Dr. R. Basani for providing plasmid. We are grateful to Dr. Dovie Wylie for her excellent language assistance.

REFERENCES

1. Kawakami, T., and Galli, S. J. (2002) *Nat. Rev. Immunol.* **2,** 773–786
2. Kalesnikoff, J., and Galli, S. J. (2008) *Nat. Immunol.* **9,** 1215–1223
3. Marshall, J. S. (2004) *Nat. Rev. Immunol.* **4,** 787–799
4. Kawakami, T., and Kitaura, J. (2005) *J. Immunol.* **175,** 4167–4173
5. Kinashi, T., and Springer, T. A. (1994) *Blood* **83,** 1033–1038
6. Kitaura, J., Eto, K., Kinoshita, T., Kawakami, Y., Leitges, M., Lowell, C. A., and Kawakami, T. (2005) *J. Immunol.* **174,** 4495–4504
7. Kitaura, J., Kinoshita, T., Matsumoto, M., Chung, S., Kawakami, Y., Leitges, M., Wu, D., Lowell, C. A., and Kawakami, T. (2005) *Blood* **105,** 3222–3229
8. Bianchine, P. J., Burd, P. R., and Metcalfe, D. D. (1992) *J. Immunol.* **149,** 3665–3671
9. Oki, T., Kitaura, J., Eto, K., Lu, Y., Maeda-Yamamoto, M., Inagaki, N., Nagai, H., Yamanishi, Y., Nakajima, H., Nakajina, H., Kumagai, H., and Kitamura, T. (2006) *J. Immunol.* **176,** 52–60
10. Gurish, M. F., Tao, H., Abonia, J. P., Arya, A., Friend, D. S., Parker, C. M., and Austen, K. F. (2001) *J. Exp. Med.* **194,** 1243–1252
11. Edelson, B. T., Li, Z., Pappan, L. K., and Zutter, M. M. (2004) *Blood.* **103,** 2214–2220
12. Knight, P. A., Wright, S. H., Brown, J. K., Huang, X., Sheppard, D., and Miller, H. R. (2002) *Am. J. Pathol.* **161,** 771–779

Downloaded from www.jbc.org at KOKURITSU KOKUSAI IRYO CT, on May 7, 2010

13. Shattil, S. J., and Newman, P. J. (2004) *Blood* **104,** 1606–1615
14. Emambokus, N. R., and Frampton, J. (2003) *Immunity* **19,** 33–45
15. Eto, K., Murphy, R., Kerrigan, S. W., Bertoni, A., Stuhlmann, H., Nakano, T., Leavitt, A. D., and Shattil, S. J. (2002) *Proc. Natl. Acad. Sci. U.S.A.* **99,** 12819–12824
16. Kieffer, N., Fitzgerald, L. A., Wolf, D., Cheresh, D. A., and Phillips, D. R. (1991) *J. Cell Biol.* **113,** 451–461
17. Suehiro, K., Smith, J. W., and Plow, E. F. (1996) *J. Biol. Chem.* **271,** 10365–10371
18. Berlanga, O., Emambokus, N., and Frampton, J. (2005) *Exp. Hematol.* **33,** 403–412
19. Mosesson, M. W. (2005) *J. Thromb. Haemost.* **3,** 1894–1904
20. Tang, L., Jennings, T. A., and Eaton, J. W. (1998) *Proc. Natl. Acad. Sci. U.S.A.* **95,** 8841–8846
21. Drew, A. F., Liu, H., Davidson, J. M., Daugherty, C. C., and Degen, J. L. (2001) *Blood* **97,** 3691–3698
22. Szaba, F. M., and Smiley, S. T. (2002) *Blood* **99,** 1053–1059
23. Fitzgerald, J. R., Foster, T. J., and Cox, D. (2006) *Nat. Rev. Microbiol.* **4,** 445–457
24. Loughman, A., Fitzgerald, J. R., Brennan, M. P., Higgins, J., Downer, R., Cox, D., and Foster, T. J. (2005) *Mol. Microbiol.* **57,** 804–818
25. Fitzgerald, J. R., Loughman, A., Keane, F., Brennan, M., Knobel, M., Higgins, J., Visai, L., Speziale, P., Cox, D., and Foster, T. J. (2006) *Mol. Microbiol.* **59,** 212–230
26. Lengweiler, S., Smyth, S. S., Jirouskova, M., Scudder, L. E., Park, H., Moran, T., and Coller, B. S. (1999) *Biochem. Biophys. Res. Commun.* **262,** 167–173
27. Gerber, D. J., Pereira, P., Huang, S. Y., Pelletier, C., and Tonegawa, S. (1996) *Proc. Natl. Acad. Sci. U.S.A.* **93,** 14698–14703
28. Kitaura, J., Song, J., Tsai, M., Asai, K., Maeda-Yamamoto, M., Mocsai, A., Kawakami, Y., Liu, F. T., Lowell, C. A., Barisas, B. G., Galli, S. J., and Kawakami, T. (2003) *Proc. Natl. Acad. Sci. U.S.A.* **100,** 12911–12916
29. Morita, S., Kojima, T., and Kitamura, T. (2000) *Gene Ther.* **7,** 1063–1066
30. Kitamura, T., Koshino, Y., Shibata, F., Oki, T., Nakajima, H., Nosaka, T., and Kumagai, H. (2003) *Exp. Hematol.* **31,** 1007–1014
31. Furumoto, Y., Nunomura, S., Terada, T., Rivera, J., and Ra, C. (2004) *J. Biol. Chem.* **279,** 49177–49187
32. Hata, D., Kawakami, Y., Inagaki, N., Lantz, C. S., Kitamura, T., Khan, W. N., Maeda-Yamamoto, M., Miura, T., Han, W., Hartman, S. E., Yao, L., Nagai, H., Goldfeld, A. E., Alt, F. W., Galli, S. J., Witte, O. N., and Kawakami, T. (1998) *J. Exp. Med.* **187,** 1235–1247
33. Inagaki, N., Goto, S., Nagai, H., and Koda, A. (1986) *Int. Arch. Allergy Appl. Immunol.* **81,** 58–62
34. Nagai, H., Sakurai, T., Inagaki, N., and Mori, H. (1995) *Biol. Pharm. Bull.* **18,** 239–245
35. Wong, M. X., Roberts, D., Bartley, P. A., and Jackson, D. E. (2002) *J. Immunol.* **168,** 6455–6462
36. Artis, D., Humphreys, N. E., Potten, C. S., Wagner, N., Müller, W., McDermott, J. R., Grencis, R. K., and Else, K. J. (2000) *Eur. J. Immunol.* **30,** 1656–1664
37. Honda, S., Tomiyama, Y., Shiraga, M., Tadokoro, S., Takamatsu, J., Saito, H., Kurata, Y., and Matsuzawa, Y. (1998) *J. Clin. Invest.* **102,** 1183–1192
38. Flick, M. J., LaJeunesse, C. M., Talmage, K. E., Witte, D. P., Palumbo, J. S., Pinkerton, M. D., Thornton, S., and Degen, J. L. (2007) *J. Clin. Invest.* **117,** 3224–3235
39. Flick, M. J., Du, X., Witte, D. P., Jirousková, M., Soloviev, D. A., Busuttil, S. J., Plow, E. F., and Degen, J. L. (2004) *J. Clin. Invest.* **113,** 1596–1606

Downloaded from www.jbc.org at KOKURITSU KOKUSAI IRYO CT, on May 7, 2010

Pivotal Role of Lnk Adaptor Protein in Endothelial Progenitor Cell Biology for Vascular Regeneration

Sang-Mo Kwon,* Takahiro Suzuki,* Atsuhiko Kawamoto, Masaaki Ii, Masamichi Eguchi, Hiroshi Akimaru, Mika Wada, Tomoyuki Matsumoto, Haruchika Masuda, Yoshihiro Nakagawa, Hiromi Nishimura, Kenji Kawai, Satoshi Takaki, Takayuki Asahara

Abstract—Despite the fact that endothelial progenitor cells (EPCs) are important for postnatal neovascularization, their origins, differentiation, and modulators are not clear. Here, we demonstrate that Lnk, a negative regulator of hematopoietic stem cell proliferation, controls endothelial commitment of c-kit$^+$/Sca-1$^+$/Lineage$^-$ (KSL) subpopulations of bone marrow cells. The results of EPC colony–forming assays reveal that small (primitive) EPC colony formation by CD34$^-$ KSLs and large (definitive) EPC colony formation by CD34$^{(dim)}$ KSLs are more robust in *lnk*$^{-/-}$ mice. In hindlimb ischemia, perfusion recovery is augmented in *lnk*$^{-/-}$ mice through enhanced proliferation and mobilization of EPCs via c-Kit/stem cell factor. We found that Lnk-deficient EPCs are more potent actors than resident cells in hindlimb perfusion recovery and ischemic neovascularization, mainly via the activity of bone marrow-EPCs. Similarly, *lnk*$^{-/-}$ mice show augmented retinal neovascularization and astrocyte network maturation without an increase in indicators of pathogenic angiogenesis in an in vivo model of retinopathy. Taken together, our results provide strong evidence that Lnk regulates bone marrow-EPC kinetics in vascular regeneration. Selective targeting of Lnk may be a safe and effective strategy to augment therapeutic neovascularization by EPC transplantation. (*Circ Res.* **2009;104:969-977.**)

Key Words: endothelial progenitor cell ■ lnk ■ vascular regeneration

Stem cell–related, postnatal neovascularization requires several activities of putative stem cells and their progeny, endothelial progenitor cells (EPCs), including the ability to self-renew in bone marrow (BM), commitment and differentiation into mature endothelial cells (ECs), mobilization from BM into the circulatory system, and recruitment to sites of neovascularization.[1,2] Many cytokines augment mobilization and/or recruitment of BM-derived EPCs,[3,4] including granulocyte colony-stimulating factor and granulocyte/macrophage colony-stimulating factor; angiogenic growth factors such as vascular endothelial growth factor (VEGF) and stromal cell–derived factor (SDF)-1; estrogen; and pharmaceutical drugs such as statins. However, these factors act not only on immature stem/progenitor cells but also on hematopoietic cells and mature ECs. Thus, the identification of a novel molecule that specifically regulates immature populations involved in EPC kinetics in BM is warranted.

Differentiation of progenitor cells into hematopoietic and endothelial lineage cells has been intensively investigated. During development, hemangioblastic aggregates originate from the mesodermal yolk sac, migrate to the fetal liver, and finally establish themselves in the BM. The results of a number of gene-targeting studies contribute to our understanding of functional molecules such as Scl/Tal,[5] c-kit, CD34, Runx-1,[6] and Flk-1,[7] which regulate the developmental kinetics of hemangioblasts and are also expressed in the common precursors of hematopoietic cells and ECs. Postnatal hematopoietic stem cells (HSCs) and EPCs also share common markers; however, the precise characteristics of hemangioblasts, mechanisms regulating cell growth in adults, and endothelial commitment of putative stem cells and/or common precursors for hematopoietic cells and ECs for postnatal vasculogenesis have not previously been reported.

The Lnk protein shares a pleckstrin homology domain, a Src homology 2 domain, and potential tyrosine phosphorylation sites with APS and SH-2B. It belongs to a family of adaptor proteins implicated in integration and regulation of multiple signaling events.[8] Lnk has been studied in the immune system, where Lnk regulates B cell production via negative regulation of pro–B-cell expansion.[8] Recently, Lnk was reported to play a critical role in maintaining the ability of HSCs to self-renew, in a study that based on BM c-Kit$^+$/Sca-1$^+$/Lineage (Lin)$^-$ (KSL) CD34$^-$ cells, which are

Original received December 16, 2008; revision received February 12, 2009; accepted March 17, 2009.

From the Departments of Regenerative Medicine Science (S.-M.K., M.E., M.W., H.M., K.K., T.A.) and Ophthalmology (T.S., Y.N.), Tokai University School of Medicine, Isehara; Vascular Regeneration Research Group (S.-M.K., A.K., M.I., H.A., T.M., H.N., T.A.), Institute of Biomedical Research and Innovation, Kobe; and Department of Community Health and Medicine (S.T.), Research Institute, International Medical Center of Japan, Tokyo.

*Both authors contributed equally to this work.

Correspondence to Takayuki Asahara, MD, PhD, Department of Regenerative Medicine Science, Tokai University School of Medicine, 143 Shimokasuya, Isehara, Kanagawa, Japan 259-1193. E-mail asa777@is.icc.u-tokai.ac.jp

© 2009 American Heart Association, Inc.

Circulation Research **is available at http://circres.ahajournals.org** **DOI: 10.1161/CIRCRESAHA.108.192856**

Downloaded from circres.ahajournals.org at National College of Nursing on July 24, 2009

a more immature HSC subpopulation than KSL CD34$^+$ cells.[9] Importantly, earlier studies report that expression of *lnk* is strong in immature cells, ie, c-kit$^+$/Lin$^-$ cells, as compared with relatively mature cells, ie, c-Kit$^-$/Lin$^-$ cells.[10] Accordingly, and because mouse BM-KSLs are capable of differentiating into both hematopoietic and endothelial lineage cells and contribute to postnatal vasculogenesis,[11–13] Lnk may regulate the functional kinetics of EPCs. Lnk has also been suggested to act as a negative regulator of the stem cell factor (SCF)–c-Kit signaling pathway.[10] SCF reportedly stimulates proliferation and differentiation of HSCs and mobilizes stem cell populations from BM into peripheral blood (PB) by binding with its receptor, c-Kit. The SCF–c-Kit signaling pathway also supports stem cell survival and motility.[14] Moreover, EPCs are recruited via interaction with membrane-bound c-Kit, which is highly expressed on ECs in ischemic tissue.[15] The c-Kit–positive cells recruited to ischemic tissue reconstitute the injured heart and vasculature, via to their ability to regulate the myocardial balance of angiogenic cytokines.[16]

Here, we sought to test the hypothesis that a lack of Lnk signaling may enhance postnatal neovascularization via specific control of the SCF–c-Kit–mediated regenerative potential of EPCs. We provide in vitro and in vivo evidence that Lnk plays a pivotal role in specific modulation of EPCs in terms of cell growth, commitment into endothelial lineage cell types, mobilization from BM into PB, and recruitment to ischemic sites for neovascularization.

Materials and Methods

An expanded Materials and Methods section is available in the online data supplement at http://circres.ahajournals.org.

Mice

The *lnk*$^{-/-}$ mice were generated as previously reported.[8] All animal care and experiments were conducted in accordance with the institutional guidelines of Tokai University School of Medicine, Isehara, Japan.

EPC Kinetics

EPC colony–forming assay (EPC-CFA), single cell–based EPC-CFA, mobilization of EPCs, and in vitro 5′-bromodeoxyuridine (BrdUrd) proliferation assay were performed.

In Vivo Study

Hindlimb Ischemia Model and Cell Transplantation

The mouse model of hindlimb ischemia was generated by ligating the proximal femoral artery of 8- to 10-week-old C57BL6/J or Balb/C nude mice.

BM Transplantation Model

C57BL/6J mice were exposed to a lethal dose of total body irradiation (10 Gy) and inoculated intravenously with 1×10^6 donor BM mononuclear cells (BM-MNCs).

Murine Model of Oxygen-Induced Retinopathy

Oxygen-induced retinopathy (OIR) was induced in C57/BL6 wild-type (WT) and lnk$^{-/-}$ mice.

Results

Deficiency of *lnk* Augments Endothelial Differentiation and Upregulates Cell Growth-Relating Signals in BM-KSL Subpopulations

Although a previous report has clearly shown that self-renewal of BM-CD34$^-$ KSLs for hematopoiesis is accelerated in *lnk*$^{-/-}$ mice,[9] the role of Lnk in ischemic vasculogenesis is unknown. We first examined *lnk* mRNA levels in various populations of BM cells and several organs of WT mice in the presence or absence of limb ischemia. Expression of *lnk* mRNA is strong in BM-CD34$^-$ KSLs regardless of tissue ischemia. Expression of *lnk* is moderate in BM-CD34$^+$ KSLs, a relatively differentiated population as compared with CD34$^-$ KSLs. In contrast, *lnk* expression was faint in samples from BM-MNCs, BM-Lin$^-$ cells, skeletal muscle, and spleen independently of ischemia. These results suggest that *lnk* is highly expressed in BM hematopoietic and endothelial progenitors but not in mature BM cells or other organs. The *lnk* expression levels were especially high in the immature fraction of BM-HSC/EPCs as compared to committing fractions (Figure 1a).

The pattern of expression of *lnk* suggests a role in differentiation of various subpopulations among BM-KSLs. To test this, we next compared the number of BM-KSLs and derivative subpopulations in *lnk*$^{-/-}$ and WT mice. The number of KSLs, CD34$^-$ KSLs, and CD34$^{(dim)}$ KSLs, but not CD34$^{(high)}$ KSLs, was significantly greater in *lnk*$^{-/-}$ mice than in WT. These data suggest that deletion of *lnk* results in an increase in immature subpopulations of KSLs (Figure 1b). To compare the vasculogenic commitment of BM-KSLs in *lnk*$^{-/-}$ mice versus WT, fluorescence-activated cell-sorting analysis for endothelial markers was performed. KSLs coexpressing Flk-1 or CXCR4 were more frequent in *lnk*$^{-/-}$ mice than in WT (Figure 1c). Thus, loss of *lnk* appears to promote vasculogenic commitment, resulting in an increase in the EPC pool in BM. Similarly, the number of EPCs increased in PB of Lnk-deficient mice (Figures I and II in the online data supplement).

To further confirm the role of Lnk in differentiation of KSL subpopulations into endothelial lineage cells, we performed an EPC-CFA established recently in our laboratory. KSLs and their subpopulations can form 2 types of EPC colony clusters, small (primitive) and large (definitive) EPC colony clusters. Both cluster types are positive for uptake of acetyl LDL (Ac-LDL) and for expression of an EC-specific marker, isolectin B4, as revealed by chemical staining. Additionally, both are positive for Flk-1 (VEGF receptor 2) and CD31 (platelet endothelial cell adhesion molecule-1), as revealed by immunocytochemistry (Online Figure III, a through d). Moreover, colony-derived cells express the endothelial markers Flk-1 and CD31 at high levels, as detected by flow cytometric analysis. Cells from large EPC clusters, which comprise more committed EPCs with spindle-like morphology, more frequently show Ac-LDL uptake and higher expression of Flk-1 and CD31 than cells from small EPC clusters (Online Figure III, c and d).

EPC-CFA was performed for each KSL subpopulation obtained from *lnk*$^{-/-}$ or WT mice. The number of small EPC colonies derived from CD34$^-$ KSLs was significantly greater in *lnk*$^{-/-}$ mice than in WT, whereas the number derived from CD34$^{(dim)}$ or CD34$^{(high)}$ KSLs was similar in *lnk*$^{-/-}$ and WT. In contrast, the number of large EPC colonies from CD34$^-$ KSLs was similar in both groups, whereas the number from CD34$^{(dim)}$ or CD34$^{(high)}$ KSLs was significantly higher in *lnk*$^{-/-}$ mice than WT (Figure 1d). These data suggest that Lnk deficiency increases the capacity of immature stem cells

Downloaded from circres.ahajournals.org at National College of Nursing on July 24, 2009

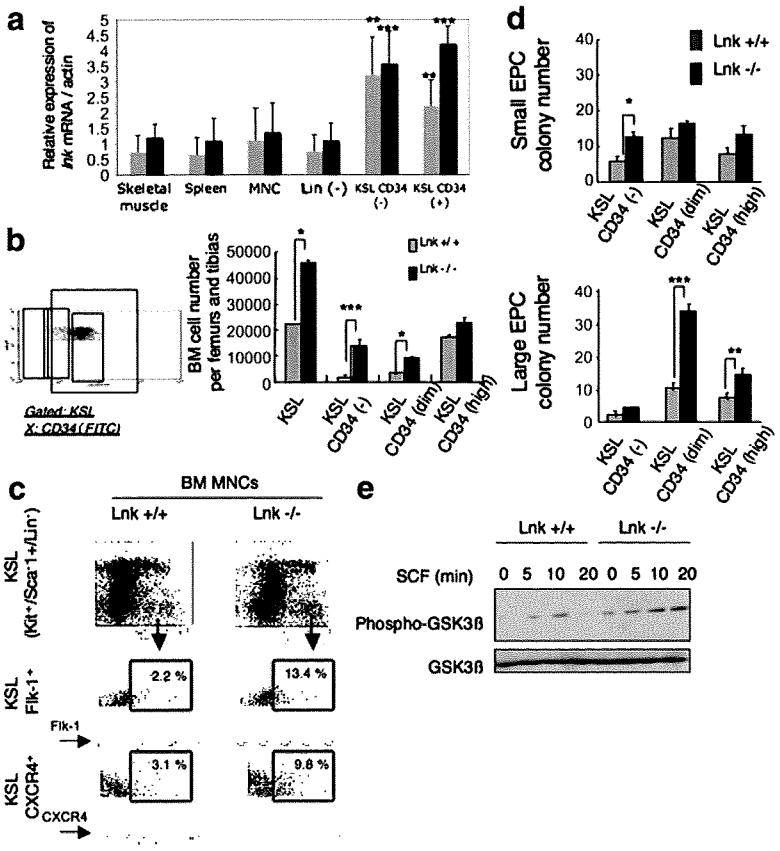

Figure 1. Lnk is pivotal for vascularization in response to ischemia. a, Relative changes in expression of *lnk* mRNA in response to ischemia. RT-PCR analysis was performed on skeletal muscle, spleen, BM-MNCs, BM-Lin$^-$ cells, and KSL subpopulations of WT mice preischemia and 3 days after hindlimb ischemia. b, Total number of KSL subpopulations by flow cytometric analysis in Lnk$^{-/-}$ mice and WT mice (n=6). c, FACS analysis of BM-KSL cells from *lnk* $^{-/-}$ and WT mice. d, EPC-CFA to evaluate vascular regeneration capacity of BM-KSL subpopulations in Lnk-deficient and WT mice. Colony number was counted 10 to 12 days after incubation of 500 cells per dish (n=4). e, Phosphorylation of GSK3β on stimulation of 100 ng/mL SCF in CD34$^{(neg)/(dim)}$ KSLs of *lnk*$^{-/-}$ and WT mice. *P<0.05, **P<0.01, ***P<0.001.

to form primitive EPCs and in the capacity of relatively mature progenitor cells to differentiate into definitive EPCs.

To compare cell growth of CD34$^-$/CD34$^{(dim)}$ KSLs from *lnk*$^{-/-}$ versus WT mice, we next analyzed SCF-dependent glycogen synthase kinase (GSK)3β phosphorylation, which is part of a signaling cascade indispensable for cell growth.[17] The level of phosphorylation of GSK3β in CD34$^-$/CD34$^{(dim)}$ KSLs was enhanced and prolonged in the *lnk*$^{-/-}$ background relative to WT. This points to an important role for Lnk in the ability of immature HSC/EPCs to cell growth, as apparently controlled by upregulation of the SCF-dependent GSK3β signaling pathway (Figure 1e).

Lnk Deficiency Upregulates Proliferation and Endothelial Commitment of EPCs Derived From KSL Populations in Culture

To explore the function of Lnk in EPC biology in terms of cell proliferation and commitment, we isolated and cultured Lin$^-$ cells, KSLs, and KSL subpopulations from WT and Lnk-deficient mice in a defined EPC culture system. In both *lnk*$^{-/-}$ and WT genetic backgrounds, KSLs in general, and CD34$^-$ KSLs and CD34$^{(dim)}$ KSLs in particular, proliferated efficiently in culture for 1 week, whereas BM-Lin$^-$ cells and CD34$^{(high)}$ KSL subpopulation cells exhibited a smaller increase in proliferation. The fold increase in cell number for KSLs, CD34$^-$ KSLs, and CD34$^{(dim)}$ KSLs was significantly greater in cells from Lnk-null mice than from WT. In contrast, the fold increase of Lin$^-$ cells and CD34$^{(high)}$ KSL subpopulation was similar in cells from *lnk*$^{-/-}$ or WT mice.

We next looked at cultured KSL subpopulations in *lnk*$^{-/-}$ and WT genetic backgrounds. The results of flow cytometric analysis reveal that cultured cells derived from CD34$^-$ KSL or CD34$^{(dim)}$ KSL subpopulations in *lnk*$^{-/-}$ mice were more frequently positive for the endothelial lineage markers Flk-1/Sca-1 and CXCR4/Sca-1 than those from WT. However, the number of cells positive for the endothelial markers among cells cultured from the CD34$^{(high)}$ KSL subpopulation was similar for *lnk*$^{-/-}$ and WT (Online Figure IV, b and c).

To determine whether EPC development from KSL subpopulations occurs at the single-cell level, we sorted single cells from each subpopulation, cultured the cells ex vivo for 1 week, and then assayed the cells using EPC-CFA and flow cytometry. EPC-CFA revealed that the number of large EPC colonies derived from a single CD34$^-$ KSL or CD34$^{(dim)}$ KSL, but not a single CD34$^{(high)}$ KSL, was significantly greater when cells were derived from *lnk*$^{-/-}$ mice. In contrast, the number of small EPC colonies derived from single cells of all subpopulations was similar in the 2 groups (Online Figure IV, d). Flow cytometry also revealed that the frequency of Sca-1$^+$/Flk-1$^+$ cells, an EPC-enriched population, among cultured cells derived from single CD34$^-$ KSLs or CD34$^{(dim)}$ KSLs, but not single CD34$^{(high)}$ KSLs, was significantly higher in *lnk*$^{-/-}$ than WT (Online Figure IV, e).

Lnk Deficiency Promotes Neovascularization In Vivo

The in vitro data above suggest that negative modulation of *lnk* gene expression may promote neovascularization in ischemic tissue. To test the in vivo effect of *lnk* deficiency,

Downloaded from circres.ahajournals.org at National College of Nursing on July 24, 2009

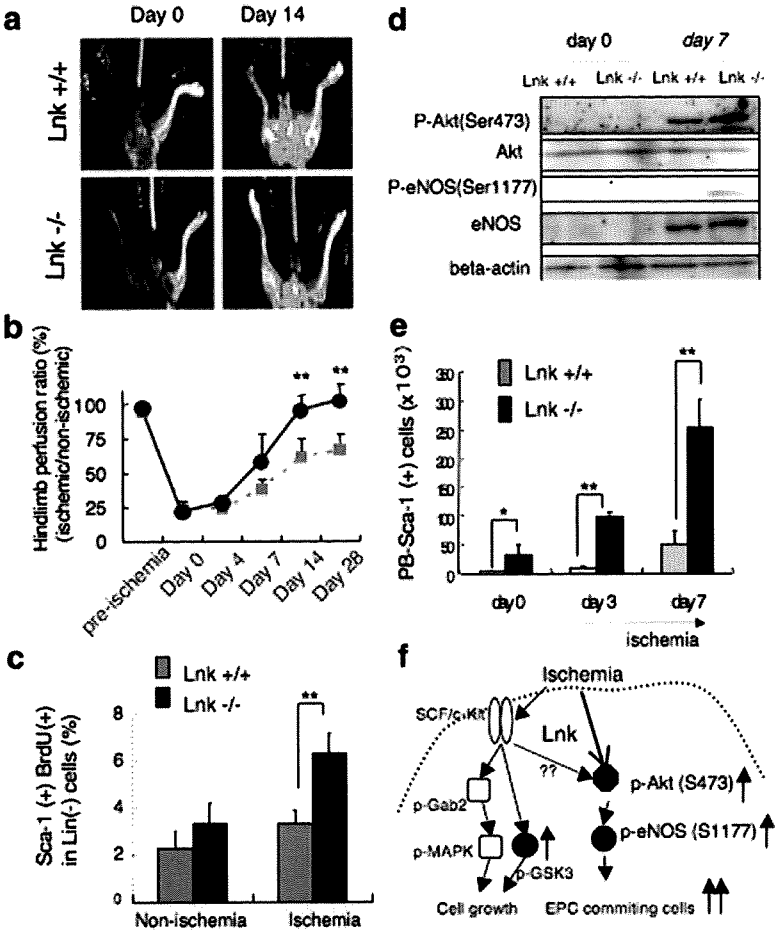

Figure 2. Neovascularization and EPC kinetics in response to hindlimb ischemia. a and b, Laser Doppler perfusion imaging (LDPI) to elucidate recovery of blood flow after ischemia in $Lnk^{-/-}$ mice and WT, expressed as the ratio of perfusion in ischemic limb to that in contralateral (nonischemic) limb (hindlimb perfusion ratio). Representative LDPI imaging (a) and serial change in hindlimb perfusion ratio (b) are shown for both groups (n=7). c, In vivo EPC proliferation activity in response to ischemia. BrdUrd incorporation into BM-derived EPCs was evaluated preischemia and 7 days after hindlimb ischemia. Percentage of $BrdUrd^+/Sca\text{-}1^+$ cells in BM Lin^- cells is shown (n=4). d, Molecular indicators of EPC differentiation in response to ischemia. Phosphorylation of Akt and eNOS in BM $Sca\text{-}1^+/Lin^-$ cells was determined by immunoblotting. P-Akt indicates phosphorylated Akt; P-eNOS, phosphorylated eNOS. e, Serial change in the number of circulating $Sca\text{-}1^+$ cells, an EPC-enriched fraction, following hindlimb ischemia in $lnk^{-/-}$ mice and WT (n=4). f, Role of Lnk in Akt/eNOS signals or GSK signals (black circle) in response to ischemia.

we generated a hindlimb ischemia model in WT and $lnk^{-/-}$ mice. Laser Doppler perfusion imaging revealed serial recovery of blood flow in the ischemic region of both groups; however, blood flow 14 and 28 days after ischemia was significantly greater in $lnk^{-/-}$ mice than in WT (Figure 2a and 2b).

To assess the mechanism of enhanced blood flow recovery in *lnk* $^{-/-}$ mice, we first compared the mitotic capacity of EPC-enriched populations in the presence or absence of hindlimb ischemia in *lnk* $^{-/-}$ and WT genetic backgrounds. The percentage of BM $Sca\text{-}1^+/BrdUrd^+$ cells in Lin^- cells without ischemia tended to be greater in *lnk* $^{-/-}$ mice than in WT, but the difference was not statistically significant. In contrast, the percentage of cycling EPCs 7 days after ischemia was significantly greater in $lnk^{-/-}$ mice than in WT. These data suggest that the proliferative activity of EPCs in response to ischemia is upregulated in the absence of Lnk activity (Figure 2c). Next, we compared the enhancement of ischemia-induced phosphorylation of Akt and of endothelial nitric oxide synthase (eNOS) levels in BM-$Sca\text{-}1^+/Lin^-$ cells in $lnk^{-/-}$ mice versus WT. The results indicate that Lnk-deficient EPCs are more potent for activation of the Akt/eNOS signaling cascade, an important pathway for EPC survival and differentiation (Figure 2d and 2f).[18] To clarify the potential of EPCs in $lnk^{-/-}$ mice for ischemic neovascularization, we used RT-PCR to compare mRNA expression of angiogenic factors and their receptors in KSL subpopulations in the presence or absence of hindlimb ischemia in $lnk^{-/-}$ and WT. In $lnk^{-/-}$ mice, genes that encode angiogenic factors or their receptors, such as *vegf*, *ang-1*, *tie-1*, and *tie-2*, were highly expressed independently of ischemic condition, whereas *ang-2*, an antagonist of TIE-2 signaling, was constitutively downregulated. In contrast, most angiogenic genes, which are weakly expressed at baseline, were upregulated postischemia in WT (Online Figure V). These data suggest that Lnk regulates the production of angiogenic factors, which in turn enhances EPC proliferation, differentiation, migration, and mobilization.

As for the kinetics of PB-EPCs, the number of $Sca\text{-}1^+$ MNCs, an EPC-enriched fraction, on days 3 and 7 after hindlimb ischemia was significantly increased in $lnk^{-/-}$ mice as compared to WT (Figure 2e). Furthermore, the number of $Sca\text{-}1^+/CD31^+$ and $Sca\text{-}1^+/Flk\text{-}1^+$ cells in PB was greater in $lnk^{-/-}$ mice as compared to WT (data not shown). These outcomes suggest that the mobilization of EPCs into circulation in response to ischemia is augmented in $lnk^{-/-}$ mice compared with WT.

A caveat to the above is that enhanced neovascularization in $lnk^{-/-}$ mice could be attributable to upregulation of angiogenic effects of resident cells as well as augmentation of BM-derived EPC kinetics. To clarify the proportional contribution of these mechanisms, we performed BM transplantation (BMT) with cells from $lnk^{-/-}$ or WT, with donor cells marked with green fluorescent protein (GFP) transplanted

Downloaded from circres.ahajournals.org at National College of Nursing on July 24, 2009

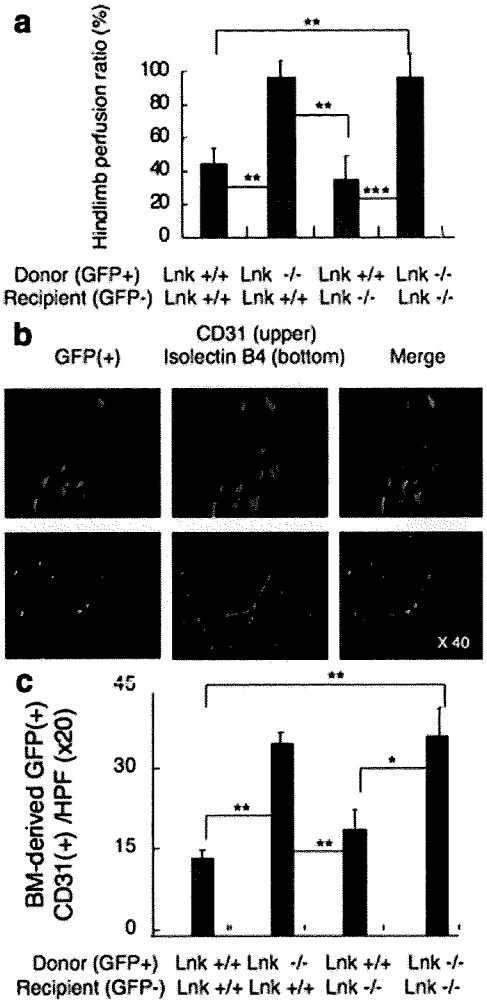

Figure 3. BM-derived EPCs predominate in blood vessel regeneration in $lnk^{-/-}$ mice. a, Ratio of donor (GFP-positive) BMTs vs host cells contributing to hindlimb perfusion 14 days after ischemia in $lnk^{-/-}$ or WT mice (n=6). b, Representative immunostaining for GFP, CD31, and isolectin B4 to identify BM-derived EPCs in ischemic tissue from WT mice perfused with BMT from $lnk^{-/-}$ mice. c, Number of BM-derived putative EPCs (ie, $GFP^+/CD31^+$ cells) in mice undergoing BMT (n=6).

into unmarked recipients. Perfusion in limb tissue at day 14 postischemia dramatically improved in WT mice that received Lnk-deficient BM cells (BMCs) as compared with WT mice receiving WT BMCs. Moreover, perfusion recovery in the hindlimb was significantly inhibited in $lnk^{-/-}$ mice receiving WT BMCs as compared with $lnk^{-/-}$ mice receiving Lnk-deficient BMCs. Importantly, hindlimb perfusion was similar in WT and $lnk^{-/-}$ mice receiving WT BMCs. Similarly, perfusion recovery was not significantly different between WT and $lnk^{-/-}$ mice receiving Lnk-deficient BMCs (Figure 3a).

Next, we detected BM-derived endothelial lineage cells incorporating into the ischemic region via immunohistochemical detection of GFP and CD31 or isolectin B4 (Figure 3b). The number of $GFP^+/CD31^+$ ECs in ischemic tissue was significantly greater in WT mice receiving Lnk-null BMCs than in those receiving WT BMCs. In addition, BM-derived ECs were more frequently observed in $lnk^{-/-}$ mice receiving Lnk-deficient BMCs than in those receiving WT BMCs. Similar to what was observed in the hindlimb perfusion analysis, the number of BM-derived ECs was equivalent in WT mice receiving Lnk-deficient BMCs and $lnk^{-/-}$ mice receiving Lnk-deficient BMCs, as well as in WT mice receiving WT BMCs and $lnk^{-/-}$ mice receiving WT BMCs (Figure 3c). These results suggest that BM-derived EPCs are indispensable for enhanced neovascularization in $lnk^{-/-}$ mice, whereas *lnk* deficiency in resident cells does not significantly contribute to ischemic neovascularization.

Lnk Deficiency Enhances EPC Kinetics in Response to Ischemia-Related Cytokines

To identify specific cytokines responsible for enhanced mobilization of BM-EPCs in $lnk^{-/-}$ mice, we investigated the effect of several potent bioactive factors on EPC mobilization in $lnk^{-/-}$ and WT genetic backgrounds. To do this, we administered G-CSF, SDF-1α, SCF, VEGF, or PBS to mice once daily over 5 days and determined the number of PB-MNCs on day 7. In both $lnk^{-/-}$ and WT mice, each factors resulted in a significant increase in the number of PB-MNCs as compared with mock treatment (PBS). The number of PB-MNCs after administration of each factor was significantly greater in $lnk^{-/-}$ mice than in WT. Notably, SCF and VEGF led to a more than 4-fold difference in PB-MNC number in $lnk^{-/-}$ versus WT (Figure 4a). The results of an EPC culture assay using PB-MNCs also revealed that the number of circulating EPCs detected after infusion of any of the factors tested significantly increased in $lnk^{-/-}$ mice as compared with WT. This difference between the 2 groups was particularly remarkable following infusion of SCF or VEGF (Figure 4b). To evaluate the scale of the Lnk-dependent SCF effect on EPC mobilization, we next looked at cell kinetics over time after SCF infusion in $lnk^{-/-}$ or WT mice. The results of serial quantification of PB-MNCs revealed a significant increase in PB-MNCs in $lnk^{-/-}$ mice that was detectable at day 2 and reached a peak on day 6 (Figure 4c). Furthermore, the results of serial FACS analysis revealed a significant increase in the PB-EPC–enriched cell fraction (ie, in $Sca\text{-}1^+/CD31^+$ or $Sca\text{-}1^+/VE\text{-}cadherin^+$ cells) that was detectable at day 0 and still observable at day 8 after initiation of SCF infusion in $lnk^{-/-}$ mice, as compared with levels in WT (Figure 4d and 4e). We next performed an in vitro proliferation assay to ask whether SCF upregulates proliferative activity of EPCs in $lnk^{-/-}$ mice as well as mobilization. In WT mice, SCF did not affect the mitotic activity of $Sca\text{-}1^+/Lin^-$ cells. In contrast, treatment with 10 ng/mL of SCF significantly augments proliferation of EPC-enriched fraction cells in $lnk^{-/-}$ mice (Figure 4f). Taken together, these data suggest that ischemia-related cytokines, in particular SCF/c-kit, are critical for both proliferation and mobilization of EPCs in $lnk^{-/-}$ mice.

Lnk-Deficient EPCs Rescue Hindlimb Ischemia Following Therapeutic Administration

To evaluate the therapeutic potential of *lnk* gene–modified EPCs in ischemic neovascularization, we isolated and intravenously transplanted BM $Sca\text{-}1^+/Lin^-$ cells from $lnk^{-/-}$ or WT mice into nude mice with hindlimb ischemia. As shown

Downloaded from circres.ahajournals.org at National College of Nursing on July 24, 2009

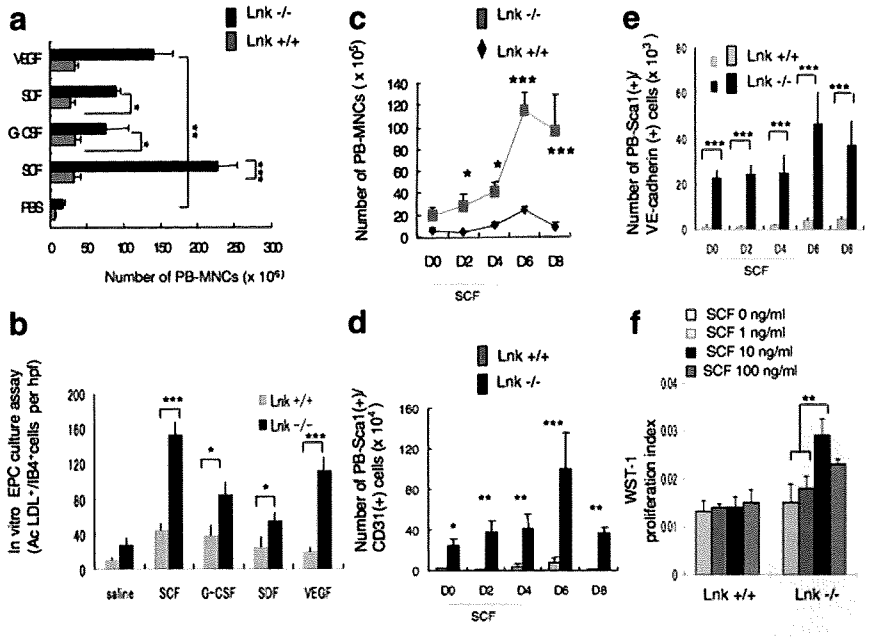

Figure 4. Effects of ischemia/angiogenesis-related cytokines on EPC kinetics are more robust in *lnk*$^{-/-}$ mice. a, Number of PB-MNCs at day 6 after initiation of VEGF, SDF-1, GCSF, SCF, or PBS in *lnk*$^{-/-}$ mice and WT (n=5). b, In vitro EPC culture assay at day 6 after initiation of VEGF, SDF-1, GCSF, SCF, or PBS in *lnk*$^{-/-}$ mice and WT (n=4). The numbers of EPCs capable of Ac-LDL uptake and positive for isolectin B4 were significantly higher in *lnk*$^{-/-}$ mice than WT. c and d, Time course of SCF-dependent mobilization kinetics in *lnk*$^{-/-}$ and WT mice (n=4 at each time point in each group). Number of circulating MNCs (c) and PB Sca-1^{+}/CD31^{+} cells (d) was serially evaluated in both groups. e, Number of Sca-1^{+}/VE-cadherin^{+} cells in response to SCF administration at each time calculated with the flow cytometric data. f, In vitro WST-1 proliferation assay using BM Sca-1^{+}/Lin^{-} cells obtained from *lnk*$^{-/-}$ and WT mice in the presence of 0, 1, 10, or 100 ng/mL of SCF. $^{*}P<0.05$, $^{**}P<0.01$, $^{***}P<0.001$.

in Figure 5a and 5b, transplantation of Lnk-null EPCs resulted in robust hindlimb perfusion as compared with WT-EPCs at equal dosing. The results of immunohistochemical analysis using the EC markers isolectin B4 and CD31 surface antigen clearly show that the capillary density at ischemic tissues is higher in animals receiving Lnk-deficient EPCs than in those receiving WT-EPCs or a mock treatment (PBS) control (Figure 5c and 5d and Online Figure VI).

Lnk Deficiency Enhances Neonatal Revascularization in OIR

We next sought to test the effect of Lnk on vascular regeneration in retinal vascular disease. To do this, we generated an animal model of neonatal retinopathy, OIR, by exposing *lnk*$^{-/-}$ or WT mice to 75% oxygen from postnatal day (P)7 to P12 (Figure 6a). In WT mice with OIR, avascular regions of the retina were readily apparent at neonatal P17. In contrast, *lnk*$^{-/-}$ mice with OIR had 4-fold smaller retinal avascular areas than WT (Figure 6b and 6c). We also observed functional regeneration of the astrocyte network, accompanied by upregulation of blood vessel regeneration, in *lnk*$^{-/-}$ mice (Online Figure VII), suggesting that enhanced neovascularization may contribute to preservation of retinal interstitial structure in the Lnk-deficient microenvironment.

Previous results suggest that enhanced angiogenesis/vasculogenesis in the retina may result in pathogenic side effects such as excess inflammation and abnormal blood vessel formation, eventually leading to retinal bleeding.[19] However,

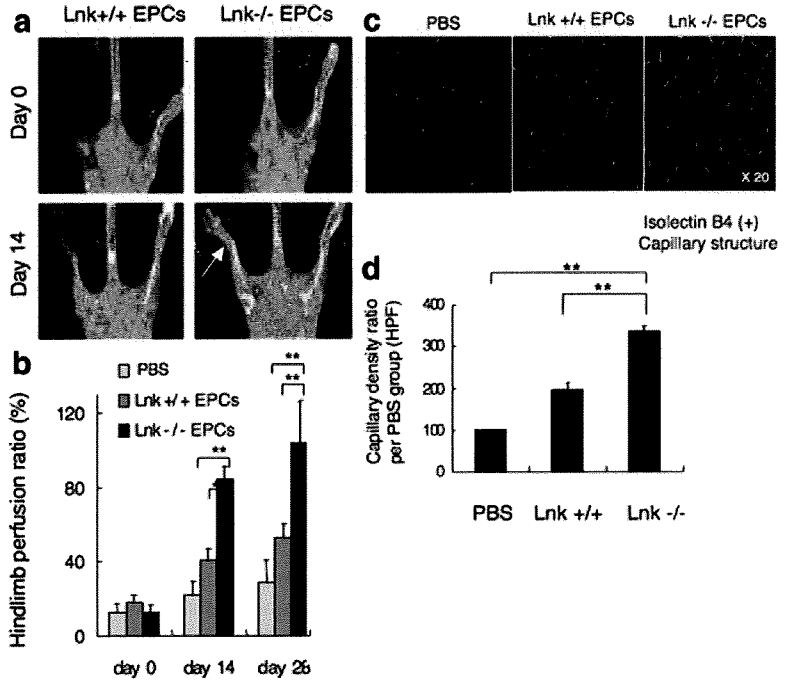

Figure 5. Lnk-deficient EPCs potently induce therapeutic neovascularization. a, Representative LDPI imaging in nude mice with hindlimb ischemia receiving BM Sca-1^{+}/Lin^{-} cells from *lnk*$^{-/-}$ or WT mice. Arrows indicate recovery of hindlimb perfusion following Lnk-deficient EPC infusion. b, Time course of hindlimb perfusion recovery in nude mice receiving mock treatment (PBS), WT-EPCs, or *lnk*$^{-/-}$ EPCs (n=7). c, Representative capillary structure revealed by chemical staining for isolectin B4 in nude mice receiving mock treatment, WT-EPCs, or *lnk*$^{-/-}$ EPCs. d, Capillary density at day 14 after hindlimb ischemia (n=7).

Downloaded from circres.ahajournals.org at National College of Nursing on July 24, 2009

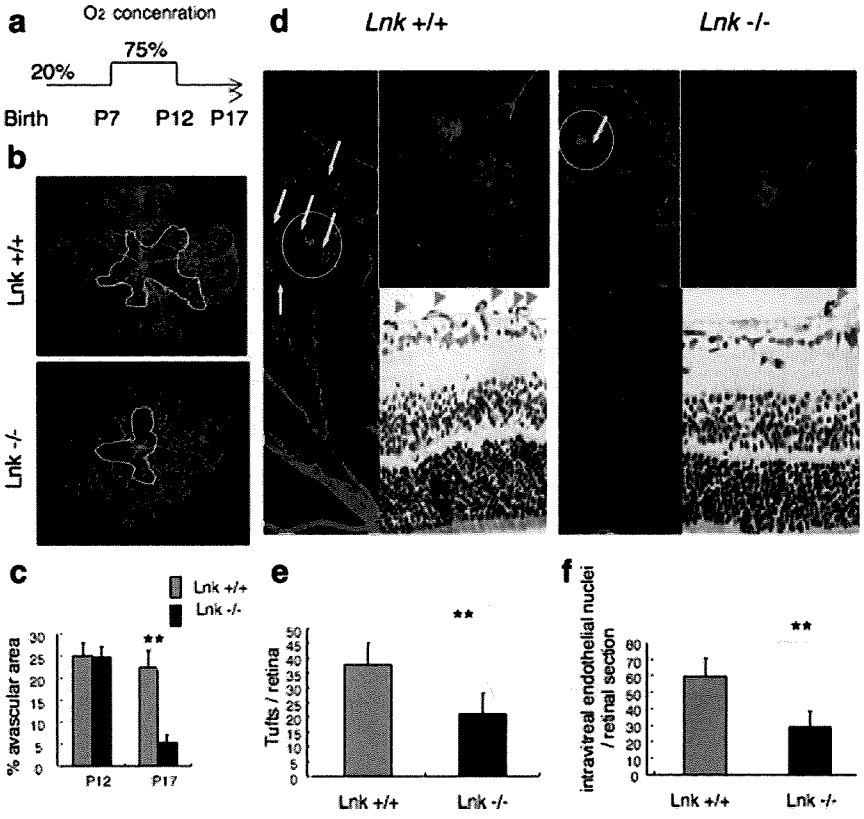

Figure 6. Augmentation of retinal neovascularization without pathogenic angiogenesis in *lnk*$^{-/-}$ mice. a, The OIR model. b, Representative immunostaining for CD31 (red) to visualize the vascular network in whole mount retina at P17 in *lnk*$^{-/-}$ and WT mice. Yellow line indicates the avascular lesion induced by hyperoxic stress. c, Percentage avascular area at P12 and P17 in *lnk*$^{-/-}$ and WT mice. d, Large images: immunostaining for CD31 (red) in P17 retinas of *lnk*$^{-/-}$ and WT mice. Arrows are tufts indicating pathogenic angiogenesis. Small images: hematoxylin/eosin staining at P17 in each group. Arrowheads indicate pathogenically formed blood vessels. e, Number of tufts per retina at P17 (n=8). f, Number of intravitreal vascular cell nuclei at P17 (n=8).

histological examination of our treated OIR model tissue revealed a smaller number of abnormally sprouting vessels in *lnk*$^{-/-}$ mice than in WT (Figure 6d through 6f). Moreover, the incidence of retinal hemorrhage at P17 was markedly lower in *lnk*$^{-/-}$ mice than in WT (Online Figures VIII and IX). These results suggest that *lnk* deficiency leads to an accelerated rate of retinal neovascularization without stimulating pathogenic blood vessel formation. To investigate this further, we isolated tissue from *lnk* deficient mice with OIR and used laser microdissection to look at the production of angiogenic growth factors in situ. Levels of VEGF, angiopoietin-1, eNOS, and leukemia inhibitory factor in vascular plexuses were significantly higher in *lnk*$^{-/-}$ mice than in WT (Figure 7b). Importantly, enhanced expression of *ang-1* may inhibit pathogenic angiogenesis by inducing the maturation of newly formed blood vessels.[20] The source of angiogenic cytokines in Lnk-null OIR is likely to be at least in part BM-derived EPCs that are recruited into the retina, as both EPCs cultured in vitro under hypoxic conditions (Online Figure X).

Discussion

The results of previous studies[12,21,22] have clearly demonstrated that BM-derived hematopoietic stem cells such as BM-KSLs serve as a reservoir of EPC origin cells in adults. In addition to having a long-term capacity for multilineage hematopoiesis, transplanted KSLs have also been shown to give rise to functional endothelial cells, even after single-cell transplantation or serial transplantation in the presence of retinal ischemic injury.[12,21] Although differentiation of hematopoietic and endothelial lineages has been intensively investigated,[5–8] molecular targets that regulate endothelial commitment of putative stem cells for postnatal vasculogenesis remain to be uncovered. Identification of molecules that control the commitment and differentiation of adult multipotent stem cells into specific lineages would be a big step toward improved therapeutic treatment in regenerative medicine. Toward identifying a modulator of endothelial development, Guthrie et al have shown that the NO pathway induces new blood vessel formation via EPCs derived from the transplanted KSLs.[22] Recently, our group reported that Jagged-1–dependent Notch signaling affects EPC bioactivities including proliferation, endothelial commitment, and mobilization from BM.[23] However, these molecules regulate multiple functions in various types of mature and immature cells. In the present study, we found a pivotal function of Lnk adaptor protein as a downstream target of the SCF–c-Kit axis that modulates vasculogenesis in BM stem cells. Lnk was most robustly expressed in BM-CD34$^-$ KSLs, which are immature putative stem cells. Lnk is also expressed at moderate levels in CD34$^+$ KSLs, a relatively differentiated stem cell type, but is not expressed in more mature cells such as BM-Lin$^-$ cells and MNCs. The results of in vitro analysis using EPC-CFA clearly indicate that Lnk deficiency results in upregulation of commitment of stem cell subpopulations into endothelial lineage cell types. Indeed, *lnk* deficiency enhances commitment of CD34$^-$ KSLs into primitive EPCs (ie, small EPC colonies). Interestingly, *lnk* deficiency also augments the activity of CD34$^{(dim)/(high)}$ KSLs for the formation of definitive EPCs (large EPC colonies). These findings suggest that Lnk may regulate not only lineage commitment but also differentiation and maturation of EPCs. The specific

Downloaded from circres.ahajournals.org at National College of Nursing on July 24, 2009

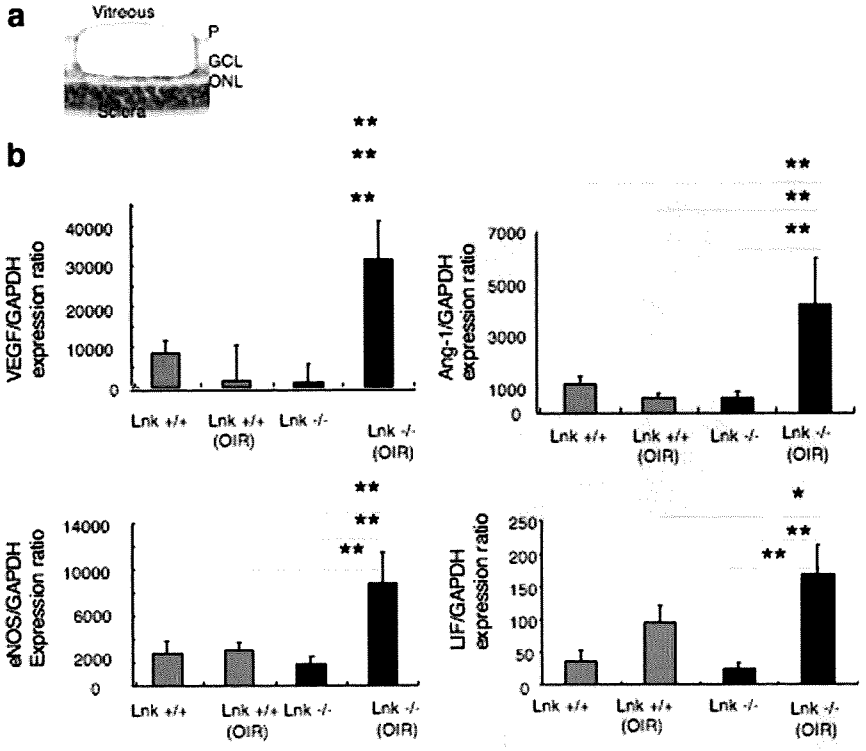

Figure 7. Augmented expression of angiogenic cytokines in *lnk*$^{-/-}$ mice. a, Representative photomicrogram showing a portion of retinal tissue dissected by laser microdissection. Counterstained with toluidine blue. P indicates periphery; GCL, ganglion cell layer; ONL, outer nuclear layer. b, Expression of angiogenic cytokines in tissue microdissected from the retina at P17 in the presence or absence of OIR induction. Expression of VEGF, Ang-1, eNOS, and leukemia inhibitory factor (LIF) mRNA was upregulated in the *lnk*$^{-/-}$ retina following OIR relative to the other groups (n=10).

expression of Lnk in stem cells and the capacity of Lnk to control lineage commitment/differentiation of BM stem cells suggest a pivotal role for Lnk as a regulator of EPCs in adults.

In addition to suggesting roles for Lnk in EPC commitment and differentiation, the results presented here also indicate that Lnk deficiency results in higher levels of proliferation of BM-KSLs and their subpopulations in vitro. Thus, we used an animal model of hindlimb ischemia to assess the effects of Lnk deficiency on EPC kinetics in vivo. Lnk deficiency results in enhanced recovery of hindlimb perfusion via upregulated proliferation of BM-derived EPCs, their enhanced mobilization activity into PB, and markedly increased recruitment into sites of ischemia. These data strongly suggest that both production of quiescent stem cells in the BM and the supply of stem cells from the BM pool for ischemic vasculogenesis may be controlled by Lnk. Furthermore, overexpression of angiogenic cytokines in Lnk-deficient KSL subpopulations suggests the importance of paracrine effects of KSL subpopulations for in situ angiogenesis as well as their autocrine effect for direct vasculogenesis. Interestingly, the results of a series of BMT experiments show that Lnk deficiency in BM-derived EPCs, but not resident EPCs/ECs, specifically augments neovascularization post hindlimb ischemia. These results provide the first direct evidence that the Lnk adapter protein plays a pivotal role in regulating the bioactivities of BM-derived EPCs for postnatal neovascularization.

Using OIR as a model for retinal damage, we also found that signs of pathogenic angiogenesis in the retina, such as tuft formation and retinal hemorrhage, were much lower in Lnk-deficient mice than in WT. Regeneration of a mature astrocyte network, along with robust neovascularization in *lnk*$^{-/-}$ mice, further supports the idea that knockdown of Lnk can have a beneficial and nonpathogenic effect in retinal vascular disease (Figure 6a through 6h and Online Figures VIII and IX). This notion may be explained by the beneficial effects of Ang-1 stimulation of vessel maturation.[22] Consistent with this, quantitative RT-PCR using microdissected retinal tissue revealed higher levels of expression of *ang-1* and other angiogenic cytokines, VEGF and eNOS, in Lnk-null mice than in WT (Figure 7b).

In conclusion, we provide strong evidence that Lnk is a definitive regulator of BM-EPC kinetics, including the ability to cell growth, endothelial commitment, mobilization, and recruitment for vascular regeneration. Selective targeting of Lnk may be a safe and effective approach to augment therapeutic neovascularization by EPC transplantation.

Acknowledgments

We thank Rie Ito for technical assistance and Sachie Ota for administrative support. We also thank all our colleagues for their helpful advice and encouragement. We appreciate assistance from the Research Center for Regenerative Medicine, the Teaching and Research Support Center, and the animal facility in the Tokai University School of Medicine and RIKEN Center for Developmental Biology.

Sources of Funding

This work was supported by the Academic Frontier Promotion Program of the Ministry of Education, Culture, Sports, Science, and Technology in Japan and a grant from the RIKEN Center for Developmental Biology.

Disclosures

None.

References

1. Asahara T, Murohara T, Sullivan A, Silver M, van der Zee R, Li T, Witzenbichler B, Schatteman G, Isner JM. Isolation of putative progenitor endothelial cells for angiogenesis. *Science.* 1997;275:964–967.

Downloaded from circres.ahajournals.org at National College of Nursing on July 24, 2009

2. Asahara T, Masuda H, Takahashi T, Kalka C, Pastore C, Silver M, Kearne M, Magner M, Isner JM. Bone marrow origin of endothelial progenitor cells responsible for postnatal vasculogenesis in physiological and pathological neovascularization. *Circ Res.* 1999;85:221–228.
3. Iwakura A, Luedemann C, Shastry S, Hanley A, Kearney M, Aikawa R, Isner JM, Asahara T, Losordo DW. Estrogen-mediated, endothelial nitric oxide synthase-dependent mobilization of bone marrow-derived endothelial progenitor cells contributes to reendothelialization after arterial injury. *Circulation.* 2003;108:3115–3121.
4. Llevadot J, Murasawa S, Kureishi Y, Uchida S, Masuda H, Kawamoto A, Walsh K, Isner JM, Asahara T. HMG-CoA reductase inhibitor mobilizes bone marrow–derived endothelial progenitor cells. *J Clin Invest.* 2001; 108:399–405.
5. Gering M, Rodaway AR, Gottgens B, Patient RK, Green AR. The SCL gene specifies haemangioblast development from early mesoderm. *EMBO J.* 1998;17:4029–4045.
6. Hirai H, Samokhvalov IM, Fujimoto T, Nishikawa S, Imanishi J, Nishikawa S. Involvement of Runx1 in the down-regulation of fetal liver kinase-1 expression during transition of endothelial cells to hematopoietic cells. *Blood.* 2005;106:1948–1955.
7. Choi K, Kennedy M, Kazarov A, Papadimitriou JC, Keller G. A common precursor for hematopoietic and endothelial cells. *Development.* 1998; 125:725–732.
8. Takaki S, Sauer K, Iritani BM, Chien S, Ebihara Y, Tsuji K, Takatsu K, Perlmutter RM. Control of B cell production by the adaptor protein lnk. Definition Of a conserved family of signal-modulating proteins. *Immunity.* 2000;13:599–609.
9. Ema H, Sudo K, Seita J, Matsubara A, Morita Y, Osawa M, Takatsu K, Takaki S, Nakauchi H. Quantification of self-renewal capacity in single hematopoietic stem cells from normal and Lnk-deficient mice. *Dev Cell.* 2005;8:907–914.
10. Takaki S, Morita H, Tezuka Y, Takatsu K. Enhanced hematopoiesis by hematopoietic progenitor cells lacking intracellular adaptor protein, Lnk. *J Exp Med.* 2002;195:151–160.
11. Bailey AS, Jiang S, Afentoulis M, Baumann CI, Schroeder DA, Olson SB, Wong MH, Fleming WH. Transplanted adult hematopoietic stems cells differentiate into functional endothelial cells. *Blood.* 2004;103: 13–19.
12. Jackson KA, Majka SM, Wang H, Pocius J, Hartley CJ, Majesky MW, Entman ML, Michael LH, Hirschi KK, Goodell MA. Regeneration of ischemic cardiac muscle and vascular endothelium by adult stem cells. *J Clin Invest.* 2001;107:1395–1402.
13. Rafii S, Lyden D. Therapeutic stem and progenitor cell transplantation for organ vascularization and regeneration. *Nat Med.* 2003;9:702–712.
14. Rafii S, Heissig B, Hattori K. Efficient mobilization and recruitment of marrow-derived endothelial and hematopoietic stem cells by adenoviral vectors expressing angiogenic factors. *Gene Ther.* 2002;9:631–641.
15. Dentelli P, Rosso A, Balsamo A, Colmenares Benedetto S, Zeoli A, Pegoraro M, Camussi G, Pegoraro L, Brizzi MF. C-KIT, by interacting with the membrane-bound ligand, recruits endothelial progenitor cells to inflamed endothelium. *Blood.* 2007;109:4264–4271.
16. Fazel S, Cimini M, Chen L, Li S, Angoulvant D, Fedak P, Verma S, Weisel RD, Keating A, Li RK. Cardioprotective c-kit+ cells are from the bone marrow and regulate the myocardial balance of angiogenic cytokines. *J Clin Invest.* 2006;116:1865–1877.
17. Trowbridge JJ, Xenocostas A, Moon RT, Bhatia M. Glycogen synthase kinase-3 is an in vivo regulator of hematopoietic stem cell repopulation. *Nat Med.* 2006;12:89–98.
18. Hiasa K, Ishibashi M, Ohtani K, Inoue S, Zhao Q, Kitamoto S, Sata M, Ichiki T, Takeshita A, Egashira K. Gene transfer of stromal cell-derived factor-1alpha enhances ischemic vasculogenesis and angiogenesis via vascular endothelial growth factor/endothelial nitric oxide synthase-related pathway: next-generation chemokine therapy for therapeutic neovascularization. *Circulation.* 2004;109:2454–2461.
19. Chen J, Somanath PR, Razorenova O, Chen WS, Hay N, Bornstein P, Byzova TV. Akt1 regulates pathological angiogenesis, vascular maturation and permeability in vivo. *Nat Med.* 2005;11:1188–1196.
20. Uemura A, Ogawa M, Hirashima M, Fujiwara T, Koyama S, Takagi H, Honda Y, Wiegand SJ, Yancopoulos GD, Nishikawa S. Recombinant angiopoietin-1 restores higher-order architecture of growing blood vessels in mice in the absence of mural cells. *J Clin Invest.* 2002;110: 1619–1628.
21. Cogle CR, Scott EW. The hemangioblast: cradle to clinic. *Exp Hematol.* 2004;32:885–890.
22. Guthrie SM, Curtis LM, Mames RN, Simon GG, Grant MB, Scott EW. The nitric oxide pathway modulates hemangioblast activity of adult hematopoietic stem cells. *Blood.* 2005;105:1916–1922.
23. Kwon SM, Eguchi M, Wada M, Iwami Y, Hozumi K, Iwaguro H, Masuda H, Kawamoto A, Asahara T. Specific Jagged-1 signal from bone marrow microenvironment is required for endothelial progenitor cell development for neovascularization. *Circulation.* 2008;118:157–165.

Downloaded from circres.ahajournals.org at National College of Nursing on July 24, 2009

STEM CELLS®
TRANSLATIONAL AND CLINICAL RESEARCH

Lnk Deletion Reinforces the Function of Bone Marrow Progenitors in Promoting Neovascularization and Astrogliosis Following Spinal Cord Injury

NAOSUKE KAMEI,[a,b,c] SANG-MO KWON,[g] CANTAS ALEV,[a,d] MASAKAZU ISHIKAWA,[b] AYUMI YOKOYAMA,[a] KAZUYOSHI NAKANISHI,[b] KIYOTAKA YAMADA,[b] MIKI HORII,[a,c] HIROMI NISHIMURA,[a] SATOSHI TAKAKI,[f] ATSUHIKO KAWAMOTO,[a] MASAAKI II,[a,c] HIROSHI AKIMARU,[a,c] NOBUHIRO TANAKA,[b] SHIN-ICHI NISHIKAWA,[c] MITSUO OCHI,[b] TAKAYUKI ASAHARA[a,c,e]

[a]Group of Vascular Regeneration, Institute of Biomedical Research and Innovation, 2-2 Minatojima-minamimachi, Chuo-ku, Kobe, Hyogo 650-0047, Japan; [b]Department of Orthopaedic Surgery, Graduate School of Biomedical Sciences, Hiroshima University, 1-2-3 Kasumi, Minami-ku, Hiroshima City, Hiroshima 734-8551, Japan; [c]Laboratory for Stem Cell Biology; [d]Laboratory for Early Embryogenesis, RIKEN Center for Developmental Biology, 2-2-3 Minatojima-minamimachi, Chuo-ku, Kobe, Hyogo 650-0047, Japan; [e]Department of Regenerative Medicine, Tokai University School of Medicine, 143 Shimokasuya, Isehara-shi, Kanagawa 259-1193, Japan; [f]Department of Community Health and Medicine, Research Institute, International Medical Center of Japan, 1-21-1 Toyama, Shinjuku-ku, Tokyo 162-8655, Japan; [g]Department of Biomedical Science, Laboratory for Vascular Medicine & Stem Cell Biology, CHA University, Seoul, Korea

Key Words. Lnk • Bone marrow • Angiogenesis • Astrogliogenesis • Spinal cord injury • Regeneration

ABSTRACT

Lnk is an intracellular adaptor protein reported as a negative regulator of proliferation in c-Kit positive, Sca-1 positive, lineage marker-negative (KSL) bone marrow cells. The KSL fraction in mouse bone marrow is believed to represent a population of hematopoietic and endothelial progenitor cells (EPCs). We report here that, in vitro, $Lnk^{-/-}$ KSL cells form more EPC colonies than $Lnk^{+/+}$ KSL cells and show higher expression levels of endothelial marker genes, including CD105, CD144, Tie-1, and Tie2, than their wild-type counterparts. In vivo, the administration of $Lnk^{+/+}$ KSL cells to a mouse spinal cord injury model promoted angiogenesis, astrogliosis, axon growth, and functional recovery following injury, with $Lnk^{-/-}$ KSL being significantly more effective in inducing and promoting these regenerative events. At day 3 following injury, large vessels could be observed in spinal cords treated with KSL cells, and reactive astrocytes were found to have migrated along these large vessels. We could further show that the enhancement of astrogliosis appears to be caused in conjunction with the acceleration of angiogenesis. These findings suggest that Lnk deletion reinforces the commitment of KSL cells to EPCs, promoting subsequent repair of injured spinal cord through the acceleration of angiogenesis and astrogliosis. STEM CELLS *2010;28:365–375*

Disclosure of potential conflicts of interest is found at the end of this article.

INTRODUCTION

The population of c-Kit-positive, Sca-1-positive, lineage marker-negative (KSL) cells in mouse bone marrow is well known to represent a fraction of hematopoietic stem/progenitor cells (HSCs) [1]. The KSL cell population is also believed to be a good source for endothelial progenitor cells (EPCs), with a portion of KSL cells able to differentiate into the endothelial lineage and to contribute to vasculogenesis in vivo [2–4]. Previous studies reported that the transplantation of human circulating CD34 positive cells believed to contain HSCs and EPCs was effective in enhancing repair and regeneration of the central nervous system (CNS) [5–7]. Other previous studies have shown that functional recovery of hindlimbs in mouse spinal cord injury (SCI) models was improved by the transplantation of mouse bone marrow KSL cells [8, 9]. However, the mechanisms for spinal cord repair promoted by KSL cell transplantation remain to be clarified.

Author contributions: N.K.: conception and design, collection and/or assembly of data, data analysis and interpretation, manuscript writing; S.M.K.: conception and design, collection and/or assembly of data; N.K. and S.M.K.: contributed equally to this work; C.A.: collection and/or assembly of data, manuscript writing; M.I., A.Y., K.N., K.Y., M.H., and M.I.: collection and/or assembly of data; H.N., S.T., and H.A.: conception and design; A.K.: manuscript writing; N.T., S.N., and M.O.: administrative support; T.A.: conception and design, administrative support.

Correspondence: Takayuki Asahara, M.D., Ph.D., Group of Vascular Regeneration, Institute of Biomedical Research and Innovation, 2-2 Minatojima-minamimachi, Chuo-ku, Kobe, Hyogo 650-0047, Japan. Telephone: +81-78-304-5772; Fax: +81-78-304-5772; e-mail: asa777@is.icc.u-tokai.ac.jp Received August 20, 2009; accepted for publication October 16, 2009; first published online in STEM CELLS *EXPRESS* January 28, 2010. © AlphaMed Press 1066-5099/2009/$30.00/0 doi: 10.1002/stem.243

Lnk is an adaptor protein expressed in KSL cells and believed to negatively regulate the key signaling pathways for the proliferation of KSL cells such as stem cell factor (SCF) signaling and thrombopoietin signaling [10–12]. In Lnk-deficient mice, the proliferation of KSL cells is upregulated and the number of KSL cells in bone marrow is increased compared to that in wild-type mice [10]. We hypothesized that the transplantation of Lnk-deficient KSL cells might be more effective in promoting repair of injured spinal cord than wild-type KSL cells. The purpose of this study was to assess the effect of Lnk-deficient KSL cell transplantation on the regeneration of injured spinal cord and to clarify the mechanisms of spinal cord repair promoted by the transplantation of KSL cells.

Materials and Methods

The Institutional Animal Care and Use Committees of RIKEN Center for Developmental Biology approved all animal procedures in this study.

Generation of Lnk-Deficient Mice

Lnk knockout mice were generated as reported previously [10, 13]. The mice used in this study were backcrossed with C57BL/6 > 10 times. They were bred and maintained at the animal facility of RIKEN Center for Developmental Biology (Kobe, Japan, http://www.cdb.riken.jp/en/index.html).

Isolation of KSL Cells

KSL cells were purified from bone marrow cells by a modification of the method reported previously [14]. Bone marrow cells were obtained from C57BL/6 mice (wild-type mice) or Lnk knockout mice. Lineage-positive cells were removed from bone marrow cells using magnetic cell separation system (BD IMag Hematopoietic Progenitor Cell Enrichment Set-DM; BD Biosciences, San Jose, CA, http://www.bdbiosciences.com). In brief, cells isolated by centrifugation with low-density solution (<1.077 g/ml) were stained with a mixture of biotinylated mouse lineage-antibodies to CD3e, CD11b, CD45R/B220, Ly-6G and Ly-6C (Gr-1), and TER-119/erythroid cells (Ly-76). Lineage-positive cells were depleted with streptavidin–magnetic beads and the use of neodymium magnets (BD IMagnet; BD Biosciences). The remaining cells were collected and further stained with phycoerythrin-conjugated anti-Sca-1 and allophycocyanin-conjugated anti-c-Kit antibodies. All antibodies were purchased from BD Biosciences. After washing, the cells were resuspended in staining medium supplemented with 7-amino-actinomycin D (7-AAD). Stained cells were analyzed by fluorescence activated cell sorting (FACS) using BD FACSAria cell-sorting system (BD Biosciences), and KSL cells were sorted. Dead cells stained with 7-AAD were excluded from analysis and sorting.

EPC Colony Forming Assay

An EPC colony forming assay established in our laboratory was performed as reported previously [15]. The number of EPC colonies was assessed after culturing single-KSL cells in a 96-well plate for 12 days in methyl cellulose-containing medium M3236 (StemCell Technologies, Vancouver, BC, Canada, http://www.stemcell.com) with 20 ng/ml SCF (Kirin, Tokyo, Japan, http://www.kirin.co.jp/english), 50 ng/ml vascular endothelial growth factor (VEGF) (R&D Systems, Minneapolis, MN, http://www.rndsystems.com), 20 ng/ml interleukin-3 (Kirin), 50 ng/ml basic fibroblastic growth factor (Wako, Osaka, Japan, http://www.wako-chem.co.jp/english), 50 ng/ml epidermal growth factor (EGF) (Wako), 50 ng/ml insulin-like growth factor-1 (IGF-1) (Wako), and 2U/ml heparin (Ajinomoto, Tokyo, Japan, http://www.ajinomoto.com). Results were expressed as mean ± SD. Statistical analysis was performed using the Mann-Whitney U test. The endothelial phenotype of the EPC colonies was confirmed by high uptake of DiI conjugated acetylated low-density lipoprotein (DiI-Ac-LDL; Biomedical Technologies, Stoughton, MA, http://www.btiinc.com), cytochemical positivity for Alexa Fluor 488 conjugated Isolectin B4 (Molecular Probes, Carlsbad, CA, http://probes.invitrogen.com), immunoreactivity for Flk-1 (Sigma, St. Louis, MO, http://www.sigmaaldrich.com), and eNOS (Sigma).

SCI Model

All surgical procedures were performed using an operating microscope (Zeiss, Oberkochen, Germany, http://www.zeiss.com). Male C57BL/6 mice (12 weeks old, weighing 24-26g) were anesthetized with an intraperitoneal injection of 400 mg/kg 2,2,2-tribromoethanol (Avertin; Sigma). After a laminectomy at the 10th thoracic spinal vertebrae, we exposed the dura mater. Spinal cord crush injury was performed by compressing the cord laterally from both sides with number 5 Dumont forceps (Fine Science Tools, North Vancouver, BC, Canada, http://www.finescience.com) as previously reported [16, 17]. In previous reports, the forceps were modified with a spacer so that a 0.4 or 0.5 mm space remained at maximal closure. These distances were selected for moderately severe injury by comparing results achieved with forceps that closed to a space of 1.0 or 0 mm. In the present study, we selected forceps without a spacer in order to make severe and reproducible injury models. Their bladders were emptied manually once a day until restoration of autonomic bladder function.

Transplantation of KSL Cells

Transplantation was performed immediately after spinal cord injury. KSL cells (1×10^5 cells in 200 μl of postburn serum (PBS)) derived from wild-type mice (WT KSL group) or Lnk knockout mice (Lnk KO KSL group) were injected intravenously. In the other injured mice, only 200 μl of PBS was injected (PBS group).

Behavioral Testing

The recovery of hindlimb motor function was assessed using the BBB locomotor rating scale [18]. Mice in each group (n = 10-12) were assessed before SCI and 1, 4, 7, 14, 21, 28, 35, and 42 days after injury. Mice were evaluated in an open field by two observers blind to the experimental condition. Results were expressed as mean ± standard error. Statistical analysis was performed using two-way repeated measures ANOVA for group × time and Scheffe's post hoc comparisons.

Electrophysiological Recording

Signal conduction in the motor pathway was assessed by motor evoked potentials (MEPs) at 6 weeks after injury as described previously [19]. Mice were anesthetized with an intraperitoneal injection of 100 mg/kg of ketamine hydrochloride, which has little effect on the MEP [20]. They were then fixed in a stereotaxic apparatus. A pair of needle electrodes was placed subcutaneously at 3 mm on each side of the vertex of the skull. The motor cortex was stimulated transcranially with 0.2 ms square wave pulses using a constant current of 50 mA. The electromuscular responses were recorded from both hamstring muscles using a commercially available system (Viking Quest; Nicolet Biomedical, Madison, WI, http://www.viasyshealthcare.com/). All signals were filtered (bandpass 0.5-2,000 Hz). To ensure reproducibility, at least five replicate responses were recorded and the recording with the highest amplitude from onset to peak of the negative deflection was used for analysis [21, 22]. Results were expressed as mean ± SD. Statistical analysis was performed using one-way ANOVA followed by Scheffe's post hoc comparisons.

Immunohistochemistry

Mice were anesthetized and transcardially perfused with 4% paraformaldehyde in PBS at day 1, 3, 14, and 42 after injury. Spinal

cords were frozen and sagittally sectioned at 16 μm on a cryostat. Sections were permeabilized with 0.3% TritonX-100 and non-specific binding sites were blocked with blocking solution (Protein Block Serum-Free; Dako, Carpinteria, CA, http://www.dako.com). Where anti-mouse IgG monoclonal antibodies were used, sections were additionally incubated with mouse IgG blocking reagent (Vector Laboratories, Burlingame, CA, http://www.vectorlabs.com). Spinal cord sections were stained with the following primary antibodies: mouse anti-nestin (1:100; BD Biosciences), rabbit anti-GFAP (1:500; Dako), rabbit anti-collagen type IV (1:200; LSL, Tokyo, Japan, http://www.cosmobio.co.jp/agency/z01.asp), rabbit anti-tyrosine hydroxylase (TH; 1:500, Chemicon, Temecula, CA, http://www.chemicon.com), rat anti-CD31 (1:100; Santa Cruz Biotechnology, Santa Cruz, CA, http://www.scbt.com), goat anti-serotonin transporter (5HT; 1:500; ImmunoStar, Hudson, WI, http://www.immunostar.com) and Alexa Fluor 488 conjugated anti-green fluorescent protein (GFP) (1:500; Molecular Probes). Secondary antibodies (1:500) used were as follows: Alexa Fluor 488 conjugated goat anti-mouse (Molecular Probes), Alexa Fluor 594 conjugated goat anti-mouse, Alexa Fluor 350 conjugated goat anti-rabbit, Alexa Fluor 488 conjugated goat anti-rabbit, Alexa Fluor 488 conjugated donkey anti-rabbit, Alexa Fluor 594 conjugated goat anti-rabbit, Alexa Fluor 594 conjugated donkey anti-rat, and Alexa Fluor 594 donkey anti-goat. Finally, except for those stained with Alexa Fluor 350 conjugated secondary antibody, the tissues were counterstained with DAPI. Immunostained sections were observed under a fluorescence microscope (BZ8000; Keyence, Osaka, Japan, http://www.keyence.com).

For the quantitative assessment of axons, the area of TH^+ or $5HT^+$ axons at two levels (caudal region adjacent to the epicenter and 5 mm caudal to the epicenter) was measured using ImageJ software as previously described [23, 24]. The diameter, number, and area of $CD31^+$ vessels, the number of $GFAP^+$ cells, GFAP negative area, and Collagen type IV^+ area were also measured by ImageJ for quantitative assessment [25, 26]. Results were expressed as mean ± SD. Statistical analysis was performed using the Mann-Whitney U test (in the case of comparison between only two groups) or one-way ANOVA followed by Scheffe's post hoc comparisons (in the case of multiple comparisons).

Real-Time Polymerase Chain Reaction Analysis in KSL Cells and Injured Spinal Cord Tissues

Total RNA was obtained from $Lnk^{+/+}$ KSL cells and $Lnk^{-/-}$ KSL cells using RNeasy Mini Kit (Qiagen KK, Tokyo, Japan, http://www1.qiagen.com) according to the manufacturer's procedure. Total RNA from spinal cord tissues was also obtained as previously described [27]. At day 3 after SCI, mice were anesthetized and transcardially perfused with 15 ml of sterile RNase-free PBS. Spinal cords were rapidly dissected, and a 5 mm segment centered on the lesion was removed and homogenized in Trizol (Invitrogen, Carlsbad CA, http://www.invitrogen.com). RNA was isolated according to the manufacturer's protocol. After the first-strand cDNA was synthesized with the use of PrimeScript RT reagent Kit (TaKaRa, Otsu, Japan, http://www.takara.co.jp), real-time quantitative reverse transcription-polymerase chain reaction (RT-PCR) was performed with ABI Prism 7,700 (Applied Biosystems, Foster City, CA, http://www.appliedbiosystems.com) using SYBR Green Master Mix reagent (Applied Biosystems) according to the manufacturer's protocol. The relative mRNA expression in each gene was normalized to the expression level of glyceraldehyde-3-phosphate dehydrogenase (GAPDH). In this method of calculation, expression level of GAPDH was reduced to 10,000. Results were expressed as mean ± SD. Statistical analysis was performed using the Mann-Whitney U test (in the case of comparison between only two groups) or one-way ANOVA followed by Scheffe's post hoc comparisons (in the case of multiple comparisons). Each primer sequence is shown in supporting information Table 1.

Results

EPC Colony Forming Units from KSL Cells

Flow cytometric analysis revealed that the ratio of $c\text{-}Kit^+$ and $Sca\text{-}1^+$ cells in the $lineage^-$ bone marrow mononuclear cell fraction isolated from Lnk knockout mice (21.8 ± 2.0%) was significantly higher than in control wild-type mice (7.7 ± 3.1%), as already shown in our previous report (Fig. 1A) [10]. To evaluate the ability of KSL cells to function as EPCs in vitro, KSL cells derived from wild-type as well as Lnk knockout mice were analyzed by EPC colony-forming assay (Fig. 1B, 1C) [15]. EPC colonies formed from KSL cells exhibited endothelial properties, including uptake of acetylated low-density lipoprotein conjugated with DiI (DiI-acetyl LDL), chemical reactivity for Isolectin B4, and immunoreactivity for vascular endothelial growth factor (VEGF) receptor-2 (Flk-1) and endothelial nitroxide synthase (eNOS) (Fig. 1B). To assess colony formation from a single cell, KSL cells were cultured in 96-well plates (single cell per well). The average number of EPC colonies per plate from $Lnk^{-/-}$ KSL cells was significantly greater than from $Lnk^{+/+}$ KSL cells (Fig. 1C). These findings suggest that Lnk deletion increased the ability of KSL cells to function as EPCs in vitro.

Gene Expression Profiles in KSL Cells

The mRNA expressions of endothelial lineage markers, stem/progenitor cell mobilization factor receptors, growth factors, and cytokines were analyzed using quantitative real-time PCR (Fig. 2). The mRNA expression level in each gene was normalized to the expression level of GAPDH. In the assessment of endothelial lineage markers, the expression levels of endoglin (CD105), vascular endothelial-cadherin (VE-cadherin, CD144), Tie-1, and Tie-2 in $Lnk^{-/-}$ KSL cells were significantly higher than in $Lnk^{+/+}$ KSL cells (Fig. 2A). In the assessment of receptors for stem/progenitor cell mobilization factors, c-Kit was highly expressed compared to VEGF receptor-1 (Flt-1), Flk-1, and CXC chemokine receptor four, and the expression level of c-Kit in $Lnk^{-/-}$ KSL cells was significantly higher than in $Lnk^{+/+}$ KSL cells (Fig. 2B). In the assessment of growth factors and cytokines, comparatively low level expressions of VEGF-C, placenta growth factor (PlGF), insulin-like growth factor one (IGF1), IGF2, brain-derived growth factor (BDNF), stem cell factor (SCF), and stromal cell-derived factor one (SDF1) were observed, together with a high level of expression of angiopoietin one (Ang1). The expression level of Ang1 and SCF in $Lnk^{-/-}$ KSL cells was significantly higher than in $Lnk^{+/+}$ KSL cells (Fig. 2C).

Functional Recovery Following Spinal Cord Injury

To assess the functional capacity of KSL cells for the treatment of injured spinal cord, PBS, $Lnk^{+/+}$ KSL cells, as well as $Lnk^{-/-}$ KSL cells were administered intravenously to SCI models of wild-type mice just after injury (PBS group, WT KSL group, and Lnk KO KSL group). The recovery of hind-limb function was assessed by using the BBB locomotor rating scale [18]. The sham control mice had scores of 21 in the BBB locomotor rating scale. All mice in PBS group, WT KSL group, and Lnk KO KSL group had a score of 21 (maximum score) before SCI, with the score being reduced to 0 at 1 day after SCI (n = 10-12 per group). Significant group effects were identified with repeated measures ANOVA ($p <$ .0001 group, time and group × time interaction). The BBB

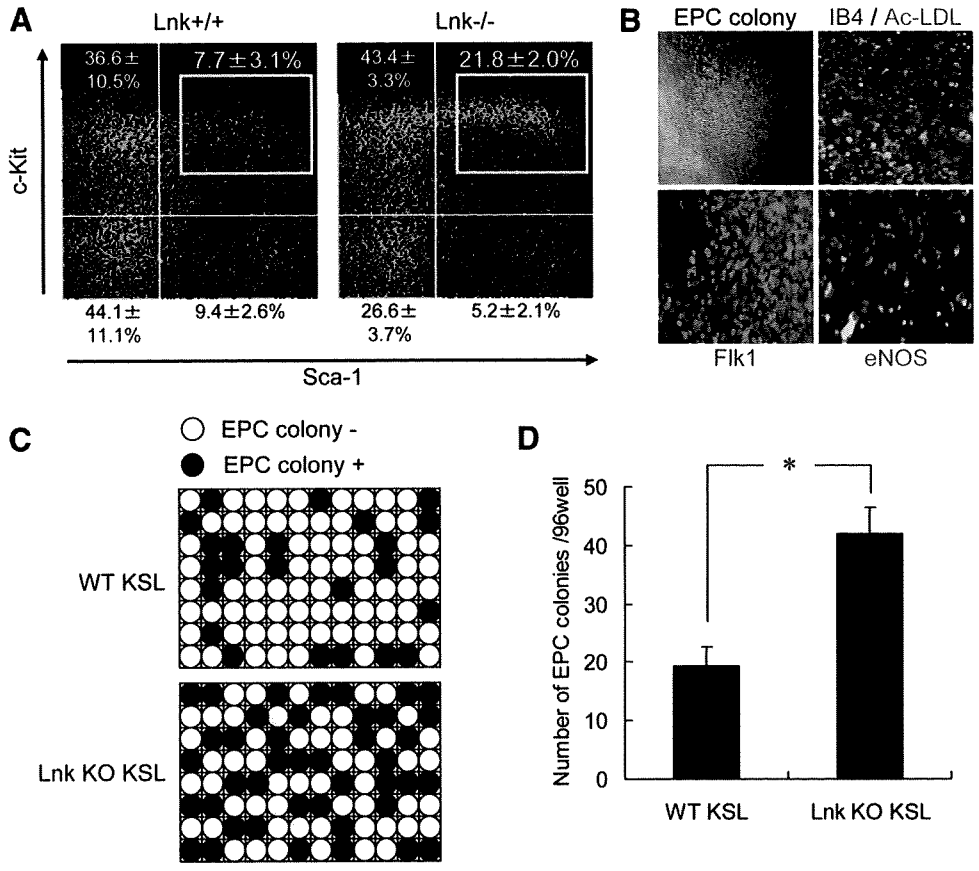

Figure 1. **(A)**: Flow cytometric analysis. Expression of c-Kit and Sca-1 in Lineage$^-$ bone marrow mononuclear cells from wild-type mouse and Lnk knockout mouse. **(B)**: Pictures of EPC colonies. Endothelial character of EPC colony cells was confirmed by uptake of DiI-acetyl LDL, chemical reactivity to Isolectin B4, and immunoreactivity for Flk-1 and eNOS. **(C, D)**: EPC colony forming assay in bone marrow KSL cells from wild-type mice (WT KSL) and Lnk knockout mice (Lnk KO KSL). Schematic diagrams of representative EPC colony forming patterns **(C)** and graph of the number of EPC colonies per 96-well plate **(D)**. *, Significant difference, $p < .05$. Abbreviations: Ac-LDL, acetylated low-density lipoprotein; eNOS, endothelial nitroxide synthase; EPC, endothelial progenitor cell; KO, knockout; KSL, c-Kit positive, Sca-1 positive, lineage marker-negative; WT, wild-type.

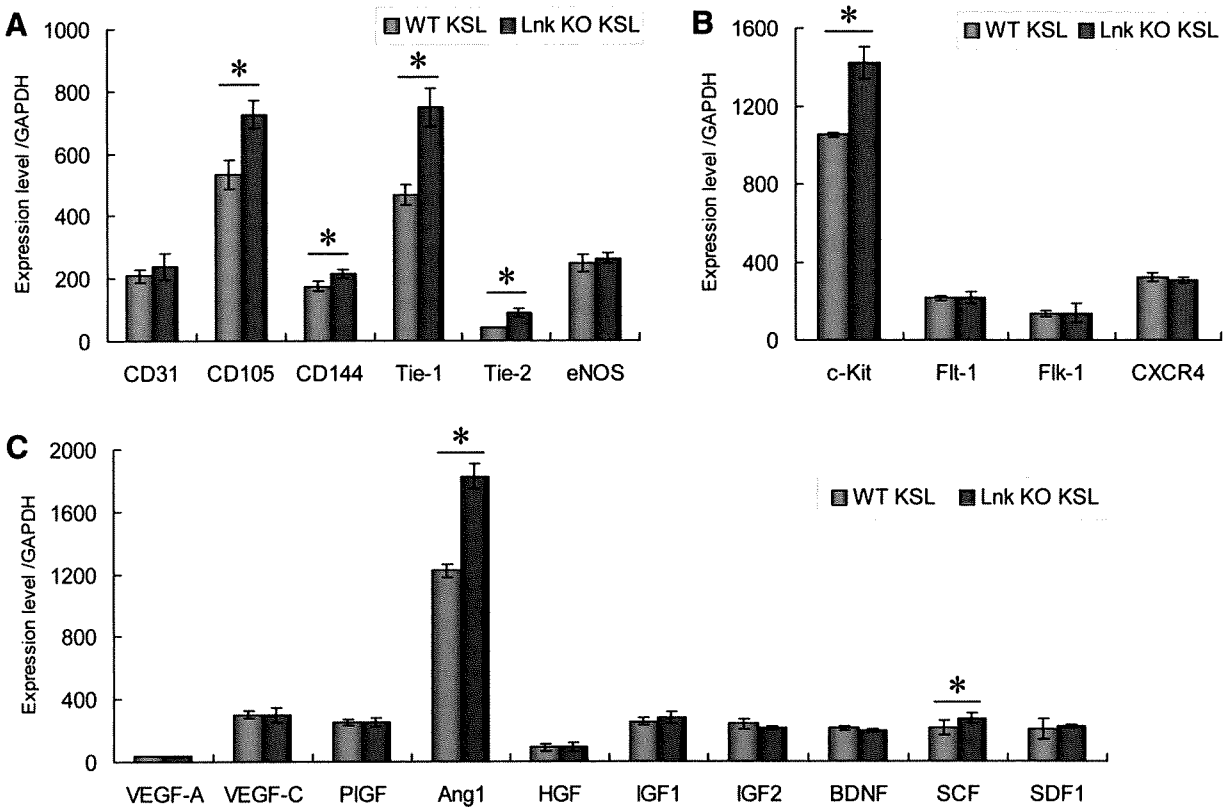

Figure 2. Gene expression profiles of bone marrow KSL cells from wild-type mice (WT KSL) and Lnk knockout mice (Lnk KO KSL) measured by real-time polymerase chain reaction. **(A)**: mRNA expressions of endothelial lineage markers, including CD31, CD105, CD144, Tie-1, Tie-2, and eNOS. **(B)**: mRNA expressions of receptors for stem/progenitor cell mobilization factors, including c-Kit, Flt-1, Flk-1, and CXCR4. **(C)**: mRNA expressions of growth factors and cytokines, including VEGF-A, VEGF-C, PlGF, Ang1, HGF, IGF1, IGF2, BDNF, SCF, and SDF1. *, Significant difference, $p < .05$. Abbreviations: Ang, angiopoietin; BDNF, brain-derived growth factor; CXCR, CXC chemokine receptor; eNOS, endothelial nitroxide synthase; GAPDH, glyceraldehyde-3-phosphate dehydrogenase; HGF, hepatocyte growth factor; IGF, insulin-like growth factor; KO, knockout; KSL, c-Kit positive, Sca-1 positive, lineage marker-negative; PlGF, placenta growth factor; SCF, stem cell factor; SDF, stromal cell-derived factor; VEGF, vascular endothelial growth factor; WT, wild-type.

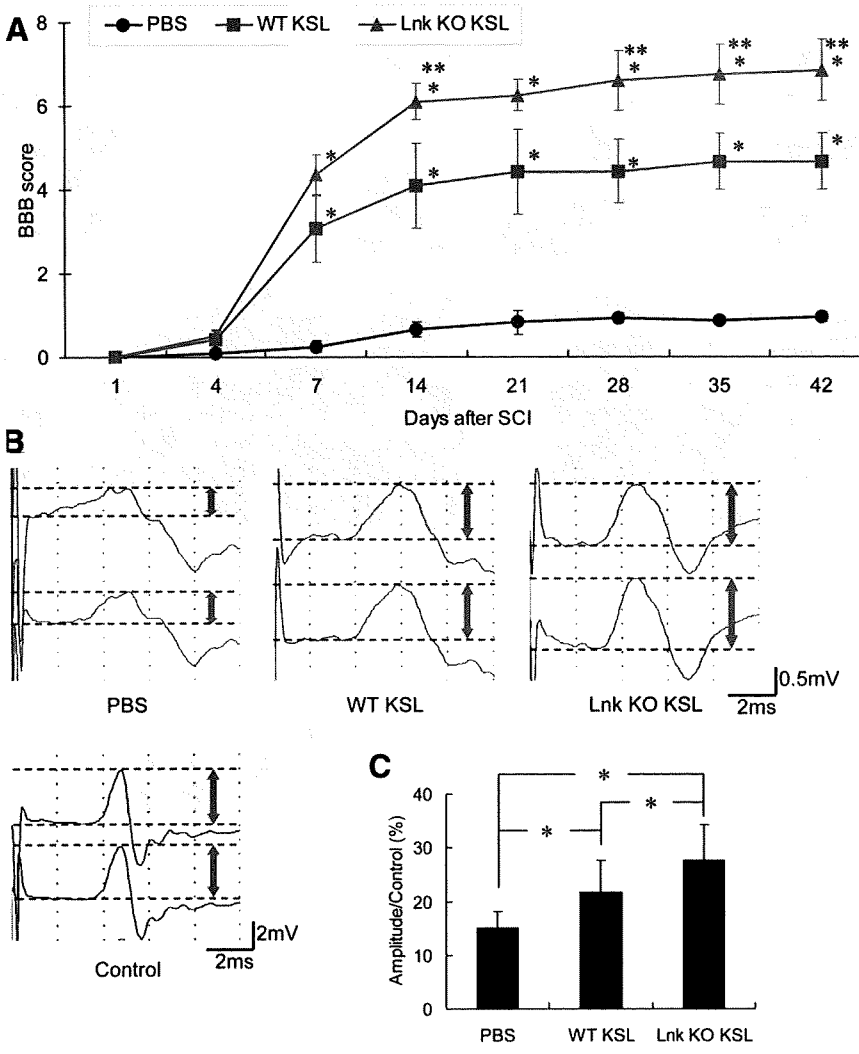

Figure 3. Assessment of functional recovery following spinal cord injury (n = 10-12). (**A**). Time course of functional recovery of limbs assessed using BBB locomotor rating scale. Significantly higher than * PBS group and ** WT KSL group, $p < .05$. (**B**). Representative motor evoked potential (MEP) waves at 6 weeks after injury. Amplitudes from onset to peak of the negative deflection were measured. (**C**): Relative ratio of MEP amplitudes to before injury. *, Significant difference, $p < .05$. Abbreviations: KO, knockout; KSL, c-Kit positive, Sca-1 positive, lineage marker-negative; PBS, postburn serum; SCI, spinal cord injury; WT, wild-type.

score in the WT KSL group and Lnk KO KSL group was significantly higher than in the PBS group at day 7 or later after SCI. In addition, the BBB score in the Lnk KO KSL group was significantly higher than in the WT KSL group at days 14, 28, or later after SCI (Fig. 3A). Hindlimb motor function while walking at days 1 and 28 after injury is shown in supporting information movies.

To assess functionality and recovery of descending pathways from the forebrain to the hindlimb motor neuron pool, transcranial electric motor evoked potentials (MEPs) were monitored in the hamstring muscles as previously reported [19]. Before SCI, MEPs were detected with an amplitude of 8.1 ± 2.0 mV (Pre-SCI; data not shown). At 6 weeks after SCI, the amplitude of MEPs in the PBS group, WT KSL group, and Lnk KO KSL group were 15.0 ± 3.1%, 21.6 ± 5.9%, and 27.7 ± 6.5% of the Pre-SCI values, respectively. The amplitude in the WT KSL group and Lnk KO KSL group was significantly higher than in the PBS group. Additionally, the amplitude in the Lnk KO KSL group was significantly higher than in the WT KSL group (Fig. 3B, 3C). These data indicate that transplantation of KSL cells facilitated the improvement of spinal cord function and that Lnk deletion enhanced the potential of KSL cells to improve the function of injured spinal cord even further.

Incorporation of Transplanted KSL Cells

To assess the incorporation of KSL cells systemically administered into mice with an injured spinal cord, KSL cells derived from GFP transgenic wild-type as well as Lnk knockout mice were administered to SCI models (n = 6/group). Spinal cord sections at 1, 3, and 14 days after SCI were analyzed under a fluorescence microscope (Fig. 4). At 1 day after SCI, GFP positive cells were detected only at the edge of spinal cord tissues around the injury site both in the WT KSL (Fig. 4B) and the Lnk KO KSL groups (Fig. 4C), although no cells were detected in the PBS group (Fig. 4A). At 3 days after SCI, GFP positive cells were detected in the spinal cord parenchyma around the injury site. A large portion of GFP^+ cells were incorporated into the platelet endothelial cell adhesion molecule-1 (PECAM-1, CD31) positive vessels or located along the $CD31^+$ vessels both in the WT KSL (Fig. 4D) and Lnk KO KSL groups (Fig. 4E). The number of GFP^+ cells in the Lnk KO KSL group was significantly greater than in the WT KSL group (Fig. 4F). At 14 days after SCI, no GFP^+ cells were observed in the spinal cord tissues from any of the groups (data not shown). Assessment of mRNA expression of stem/progenitor cell mobilization factors in the spinal cord tissues at day 3 after SCI (n = 3 per group) revealed that there was no significant difference in the

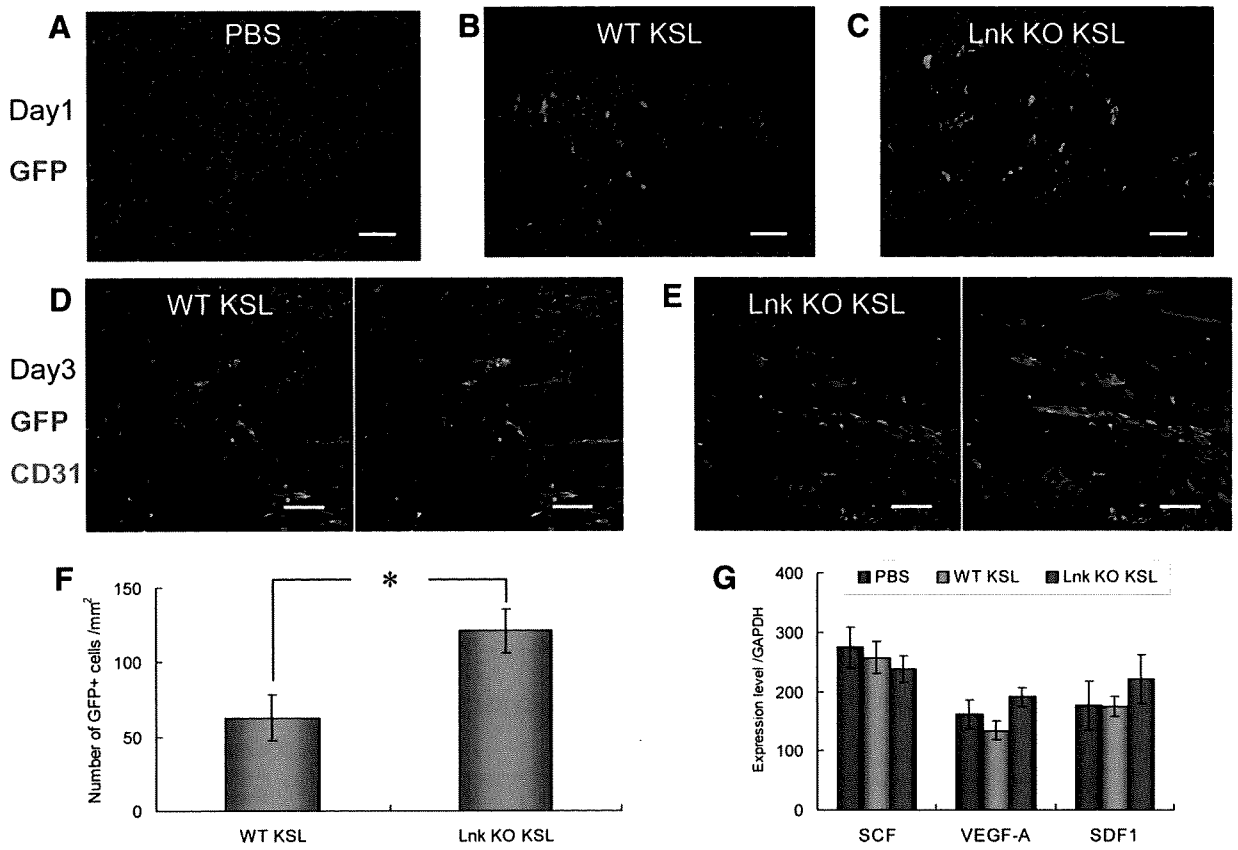

Figure 4. Incorporation of transplanted GFP$^+$ KSL cells into spinal cord. (**A**--**C**): Spinal cord tissues immunostained with anti-green fluorescent protein (GFP) antibodies at day 1 after injury in PBS group (**A**), WT KSL group (**B**), and Lnk KO KSL group (**C**). (**D**, **E**): Spinal cord tissues immunostained with anti-GFP and anti-CD31 antibodies at day 3 after injury in WT KSL group (**D**) and Lnk KO KSL group (**E**). (**F**): Number of GFP$^+$ cells incorporated into spinal cord at day 3 after injury. (**G**): mRNA expressions of stem/progenitor cell mobilization factors, including stem cell factor, vascular endothelial growth factor-A, and stromal cell-derived factor one in spinal cord tissues at day 3 after injury. *, Significant difference, $p < .05$. Scale bar: (**A**–**E**): 50 μm. Abbreviations: GFP, green fluorescent protein; KO, knockout; KSL, c-Kit positive, Sca-1 positive, lineage marker-negative; PBS, postburn serum; WT, wild-type.

expression levels of SCF, VEGF, and SDF1 among the PBS, WT KSL, and Lnk KO KSL groups (Fig. 4G).

Neovascularization and Astrogliosis in Injured Spinal Cord

At day 3 after SCI, the diameter, number, and area of CD31$^+$ vessels were analyzed in the region adjacent to the epicenter of the injury site (dotted-line box in Fig. 4A). The mean diameter, number, and area of vessels in the WT KSL and Lnk KO KSL groups were significantly larger than in the PBS group. Although the number of vessels in the Lnk KO KSL group was similar to that in the WT KSL group, the mean diameter and area of vessels in the Lnk KO KSL group were significantly greater than those in the WT KSL group (Fig. 5A, 5B). At day 3 after SCI, reactive astrocytes were stained with antibodies against glial fibrillary acidic protein (GFAP; green in Fig. 5C) and nestin (red in Fig. 5C). Reactive astrocytes were detected around the injury site (dotted-line box in Fig. 5C) both in WT KSL and Lnk KO KSL groups, whereas they were rare in the PBS group (Fig. 5C). In Figure 5C, some GFAP$^+$ astrocytes in the sections are nestin negative. Because nestin is a marker for immature cell, we speculate that GFAP$^+$ and nestin$^-$ cells might involve remaining astrocytes after injury or matured reactive astrocytes. A large portion of reactive astrocytes were distributed along large CD31$^+$ vessels (Fig. 5D). The number of reactive astrocytes in the WT KSL and Lnk KO KSL groups was significantly greater than that in the PBS group. Additionally, the number of reactive astrocytes in the Lnk KO KSL group was significantly greater than that in the WT KSL group (Fig. 5E). These findings suggest that transplantation of KSL cells promotes angiogenesis and astrogliosis in the acute phase of spinal cord injury and that Lnk deletion strengthens the function of KSL cells in promoting these events.

At day 14 after injury, morphological changes of CD31$^+$ vessels at the epicenter of the injury site (epicenter zone; area 1 in Fig. 5A) were different from ones of the laterally-damaged region (lateral zone; area 2 in Fig. 5A). Therefore, the diameter, number, and area of CD31$^+$ vessels in these regions were assessed separately ($n = 6$ per group). In the epicenter zone, a chaotic vascular architecture with large vessels adjacent to small vessels was observed in the PBS group (Fig. 6C). In contrast, the diameter and distribution of vessels in the WT KSL and Lnk KO KSL groups resembled the distribution found in the gray matter of normal spinal cord (Fig. 6B, 6C). The mean diameter, number, and area of CD31$^+$ vessels in the PBS group were significantly greater than in the normal spinal cords, the WT KSL, and the Lnk KO KSL groups (Fig. 6E–6G). Although there was no significant difference in the mean diameter of vessels between the WT KSL and Lnk KO KSL groups, the mean diameter of vessels in the WT KSL group was significantly larger than in the normal spinal cord, whereas the mean diameter of vessels in the Lnk

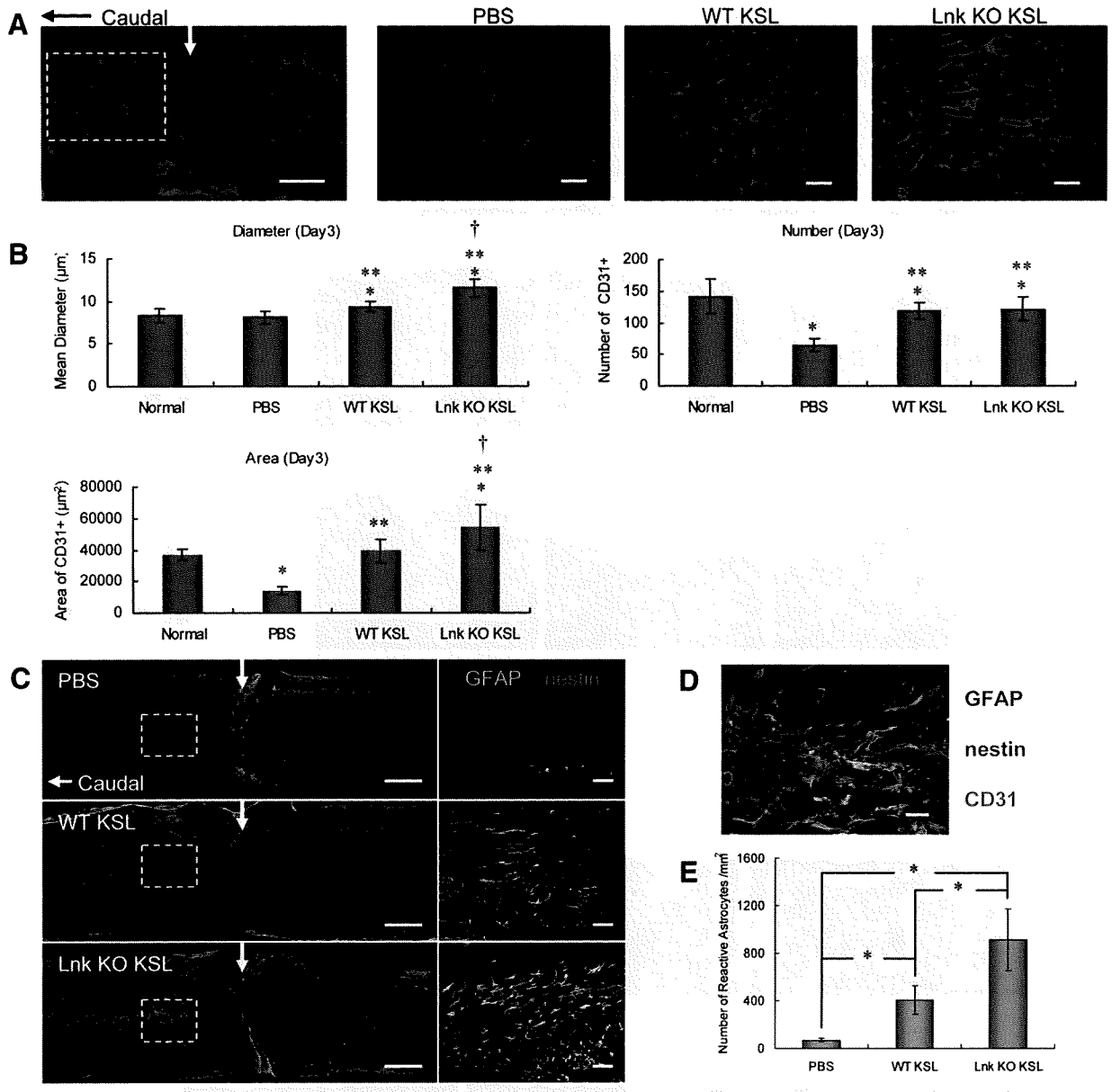

Figure 5. **(A)**: Spinal cord sections at day 3 after injury immunostained with CD31. Arrow indicates epicenter of injury site. **(B)**: Assessment of mean diameter, number, and area of $CD31^+$ vessels ($n = 6$). **(C)**: Spinal cord tissues at day 3 after injury immunostained with GFAP (green) and nestin (red). **(D)**: Spinal cord section at day 3 after injury immunostained with GFAP (blue), nestin (green), and CD31 (red) in Lnk KO KSL group. **(E)**: Number of $GFAP^+$ cells at day 3 after injury ($n = 6$). Significantly different from * non-injured spinal cord, ** PBS group, and † WT KSL group, $p < .05$. Scale bars: **(A)**: Large picture, 300 μm, and small pictures, 100 μm; **(C)**: Large pictures, 300 μm, and small pictures, 50 μm; **(D)**: 20 μm. Abbreviations: GFAP, glial fibrillary acidic protein; KO, knockout; KSL, c-Kit positive, Sca-1 positive, lineage marker-negative; PBS, postburn serum; WT, wild-type.

KO KSL group was not significantly different from that of the normal spinal cord (Fig. 6E). In the lateral zone, there were no obviously large vessels observed in the epicenter zone (Fig. 6D). The mean diameter of vessels in the Lnk KO KSL group was significantly larger than in the PBS group, although not significantly different from the normal spinal cord (Fig. 6E). The number of vessels in the WT KSL group was significantly less than in normal spinal cords, while the number of vessels in the Lnk KO KSL group was not significantly different from the number found in the normal spinal cords but was significantly greater than that in the WT KSL group (Fig. 6F). The area of vessels in the PBS group was significantly smaller than that in the normal spinal cord, where as the area of vessels in the Lnk KO KSL group was significantly larger than that in the PBS group and the WT KSL group (Fig. 6G). These findings suggest that the transplantation of KSL cells contributes to vascular stabilization at the epicenter of the injury site in the subacute phase of SCI and that Lnk deletion enhances the function of KSL cells for vascular stabilization in the epicenter zone even further, promoting angiogenesis in the lateral zone during the subacute phase of SCI.

At day 42 after SCI, spinal cord tissues were stained with antibodies against GFAP and collagen type IV for the assessment of glial and fibrous scar formation ($n = 6$ per group, Fig. 7). The GFAP negative area in the WT KSL group and

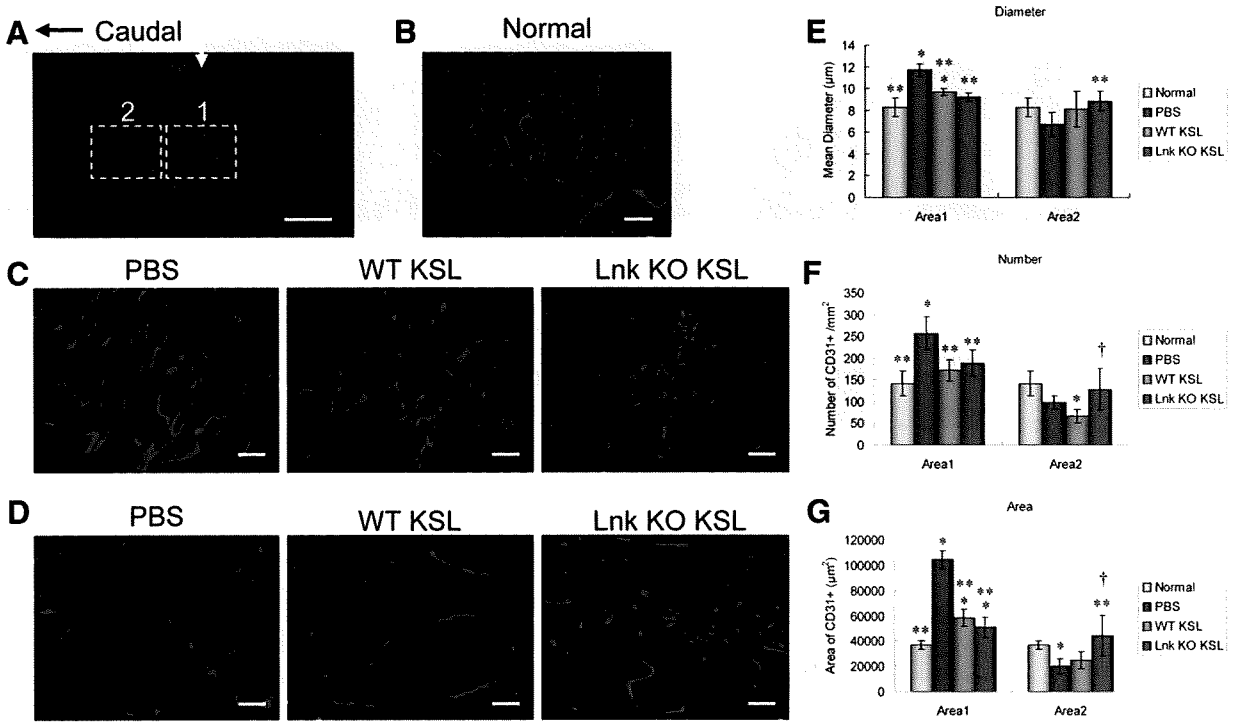

Figure 6. Immunostaining for CD31 in non-injured spinal cord and injured spinal cord at day 14 after injury. **(A)**: CD31$^+$ vessels were assessed at the epicenter of the injury site (epicenter zone, Area1) and the laterally damaged region (lateral zone, Area2). **(B)**: Gray matter in non-injured spinal cord (Normal). **(C)**: Area1 in the injured spinal cord. **(D)**: Area2 in the injured spinal cord. **(E–G)**: Quantitative assessment of vessels, including mean diameter **(E)**, number **(F)**, and area **(G)**. Significantly different from * non-injured spinal cord, ** PBS group, and †WT KSL group, $p < .05$. Scale bars: **(A)**: 300 μm; **(B–D)**: 50 μm. Abbreviations: KO, knockout; KSL, c-Kit positive, Sca-1 positive, lineage marker-negative; PBS, postburn serum; WT, wild-type.

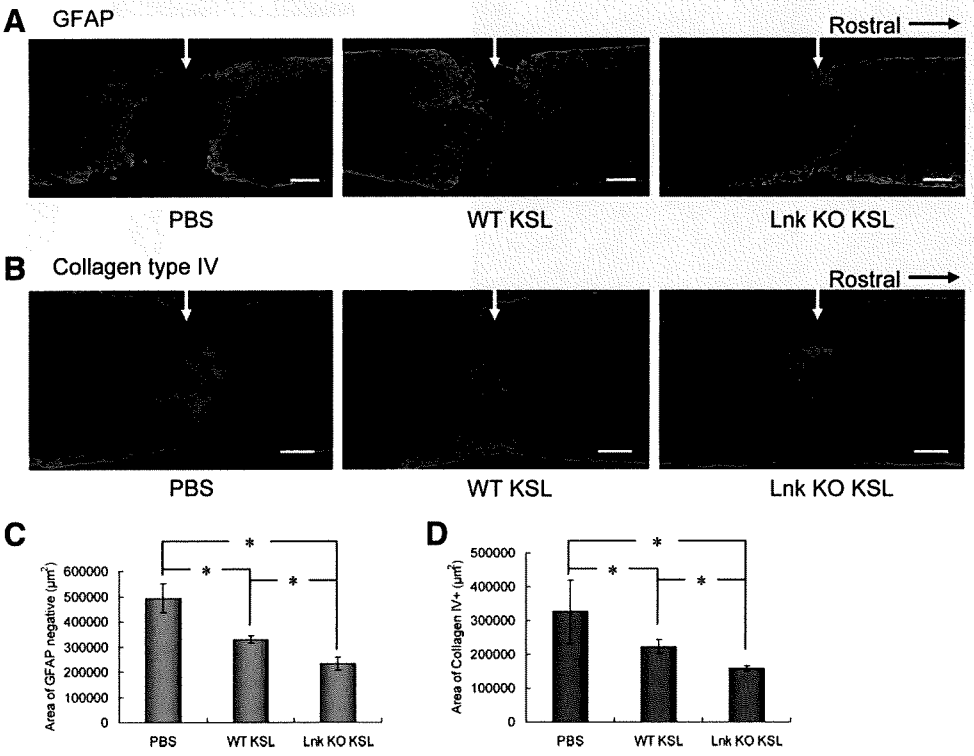

Figure 7. **(A, B)**: Spinal cord sections immunostained with GFAP **(A)** and collagen type IV **(B)** at 6 weeks after injury. **(C, D)**: Quantitative assessment of GFAP negative area **(C)** and collagen type IV$^+$ area **(D)**. * Significant difference, $p < .05$. Scale bars: **(A, B)**: 300 μm. Abbreviations: GFAP, glial fibrillary acidic protein; KO, knockout; KSL, c-Kit positive, Sca-1 positive, lineage marker-negative; PBS, postburn serum; WT, wild-type.

the Lnk KO KSL group was significantly smaller than that in the PBS group. Furthermore, the GFAP-negative area in the Lnk KO KSL group was significantly smaller than that in the WT KSL group (Fig. 7A, 7C). In the assessment of the collagen IV$^+$ area, a similar pattern compared to the GFAP-negative area was observed (Fig. 7B, 7D).

Immunohistochemical Assessment of Axons

To analyze defined subsets of descending axons, immunohistochemistry for tyrosine hydroxylase (TH; a marker for descending noradrenergic and dopaminergic axons as well as sympathetic fibers) and serotonin transporter (5HT; a marker for descending serotonergic axons) was performed as previously reported [28]. To evaluate axon growth into the injury site, quantitative assessment of axons was performed by measuring the area of immunostained axons in the caudal region adjacent to the epicenter of the injury site (dotted-line box in supporting information Fig. 1A, 1B). The area of TH^+ or $5HT^+$ axons in the WT KSL and Lnk KO KSL groups was significantly greater than that in the PBS group. In addition, the area of TH^+ or $5HT^+$ axons in the Lnk KO KSL group was significantly greater than that in the WT KSL group (supporting information Fig. 1C, 1D). A similar assessment of axons was also performed in the far caudal region (5 mm caudal to the epicenter). However, neither TH^+ axons nor $5HT^+$ axons were detected in any of the groups analyzed (data not shown).

DISCUSSION

Our findings demonstrate that the transplantation of KSL cells promotes angiogenesis and astrogliogenesis in the acute phase of SCI and vascular stabilization, reduction of fibrous scar formation, axonal growth and functional recovery in the subacute phase and later. Lnk deletion enhances the effect of KSL cell transplantation even further, promoting regenerative changes in the injured spinal cord.

Lnk Deletion Enhances the Potential of KSL Cells As EPCs

Lnk was reported to negatively regulate SCF/c-Kit signaling in B cell progenitors, hematopoietic stem/progenitor cells, and mast cells [10, 13, 29]. Lnk is furthermore considered to negatively regulate endothelial cell derived hematopoiesis during embryonic development [30]. In addition, Lnk is expressed in endothelial cells and played a role in the regulation of vascular cell adhesion molecule-1 expression in response to tumor necrosis factor-α through inhibition of the extracellular-related kinase 1/2 pathway [31, 32]. On the basis of these data, we speculate that Lnk might be involved in the differentiation and functional regulation of endothelial cells as well as endothelial progenitor cells [33]. In the present study, the mRNA expression levels of several endothelial markers in $Lnk^{-/-}$ KSL cells were higher than in $Lnk^{+/+}$ KSL cells. In addition, Lnk deletion enhanced the EPC colony forming potential of KSL cells in vitro. In vivo, the transplantation of $Lnk^{-/-}$ KSL cells further promoted angiogenesis compared to $Lnk^{+/+}$ KSL cells. These findings indicate that Lnk deletion intensified the ability of KSL cells to function as EPCs. Lnk might negatively regulate the proliferation of EPCs or the commitment of bone marrow stem cells to EPCs, although further elucidation of the role of Lnk in EPCs is needed.

Recruitment of Transplanted KSL Cells into Injured Spinal Cord

The mRNA expression level of c-Kit, which is a receptor for SCF in $Lnk^{-/-}$ KSL cells, was significantly higher than in $Lnk^{+/+}$ KSL cells. We validated this observation by showing that $Lnk^{-/-}$ KSL cells contained a bigger $c\text{-}Kit^+$ fraction than $Lnk^{+/+}$ KSL cells by flow cytometric assessment (Fig. 1A). On the other hand, no significant difference in the mRNA expression levels of SCF, VEGF, and SDF1 were observed in the injured spinal cord tissues of all three analyzed groups. SCF is believed to play an important role not only for proliferation and survival but also in the homing of hematopoietic progenitor cells [34]. Lutz et al. reported that myocardial administration of SCF-enhanced myocardial recruitment of intravenously injected bone marrow $c\text{-}Kit^+$ $lineage^-$ cells [35]. In analogy, the higher expression of c-Kit in $Lnk^{-/-}$ KSL compared to $Lnk^{+/+}$ KSL cells may explain the observed high incorporation of administered $Lnk^{-/-}$ KSL cells into the injured spinal cord.

KSL Cells Enhance the Angiogenesis in the Acute Phase of SCI

At day 3 after SCI, angiogenesis was enhanced by the transplantation of KSL cells. The mRNA expressions of several angiogenic factors, including VEGF-C, PlGF, Ang1, IGF1, IGF2, and BDNF, were observed in KSL cells. In particular, the expression level of Ang1 was strikingly higher than any of the other factors. A previous study showed that a balanced expression of Ang1 and VEGF is required for successful angiogenesis [36]. We therefore speculate that Ang1 might be a key factor for the induction and enhancement of angiogenesis after KSL cell transplantation. In addition, the expression level of Ang1 in $Lnk^{-/-}$ KSL cells was significantly higher than in $Lnk^{+/+}$ KSL cells. Overall, the high incorporation of $Lnk^{-/-}$ KSL cells into injured spinal cord together with a high expression of Ang1 in $Lnk^{-/-}$ KSL cells might be the cause for the strong induction of angiogenesis seen after $Lnk^{-/-}$ KSL cell transplantation.

KSL Cells Promote Astrogliosis Following SCI

Glial scars, formed in part by reactive astrocytes after SCI, have long been considered detrimental to the repair of injured spinal cord because glial scars or their products act as physical or chemical barriers to axonal regeneration [37–39]. However, recent studies have shown that reactive astrocytes are also important in supporting the repair of injured spinal cord [16, 25, 40]. They mentioned that reactive astrocytes are important for the repair of the blood–brain barrier and the restriction of inflammation that leads to a reduction in secondary degeneration after SCI. In addition, it has been reported that various growth factors such as nerve growth factor, brain-derived growth factor (BDNF), hepatocyte growth factor, VEGF, and fibroblast growth factor-2, which promote neuroprotection, axonal growth, and angiogenesis, are expressed in reactive astrocytes [41]. On the basis of these data from previous studies, reactive astrocytes, at least in the acute and subacute phase of SCI, might be considered beneficial to the repair of the injured spinal cord. In the present study, the transplantation of KSL cells promoted the induction of reactive astrocytes following SCI. Furthermore, Lnk deletion enhanced the effect of KSL cell transplantation promoting astrogliogenesis following SCI. Additionally, particular localization of reactive astrocytes along large vessels was observed. Recent previous studies have shown that the vascular niche is closely related to the commitment of slow-proliferating neural stem cells to fast-proliferating transit-amplifying precursors in the adult subventricular zone in homeostasis as well as during regeneration, whereas molecular mechanisms underlying this phenomenon have not been clarified [42, 43]. We therefore speculate that the promotion of angiogenesis caused by the transplantation of KSL cells enhanced astrogliogenesis through the provision of a functional vascular niche.